Instructions

Bookmarks (left column) link to the corresponding page in the booklet. You may also use Acrobat or another pdf reader's search capabilities to reach abstracts of interest.

ABSTRACTS

Table of Contents

Imaging/Population Studies Papers, Moderators: Ryo Asaoka, Ulrich Schiefer

Population Studies

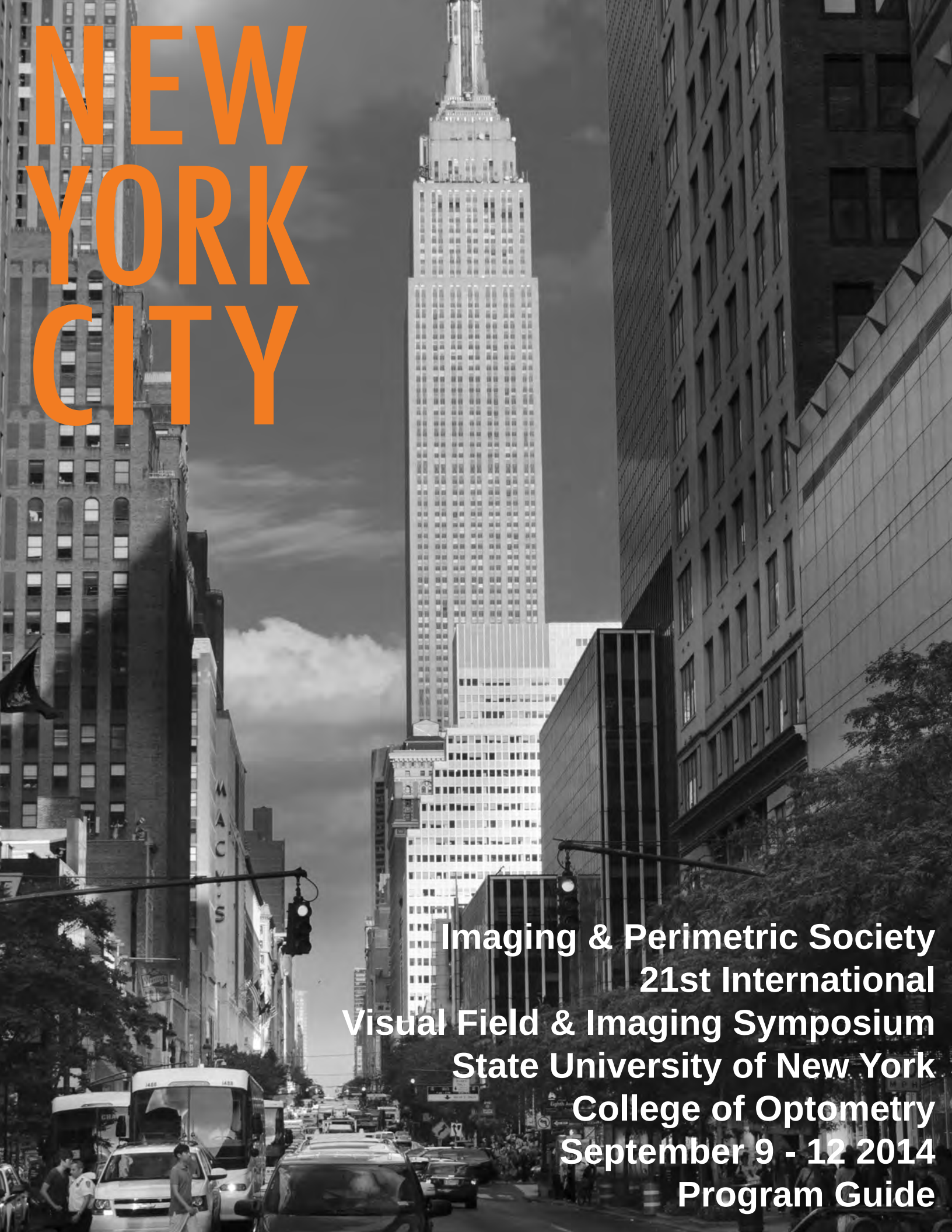
NEW
YORK
CITY
Imaging & Perimetric Society
21st International
Visual Field & Imaging Symposium
State University of New York
College of Optometry
September 9 - 12 2014
Program Guide

Psychophysics Paper Session

Sequence effects in perimetric frequency-of-seeing data

Paul H Artes,[1] F Fischl,[2] A Thal,[2] M Stewart [1]Ophthalmology and Visual Sciences, Dalhousie University, Halifax, Nova Scotia, Canada.[2]University of Applied Sciences, Aalen, Germany

Purpose: Learning- and fatigue effects are well described in perimetry, but there is little data on how patients' responses change during a test, and in response to previous stimuli. Here, we investigate such effects in frequency-of-seeing (FOS) data. Our hypothesis is that observers are less likely to respond to difficult (near-threshold) stimuli after having experienced a series of bright stimuli, and vice versa.

Design and methods: FOS data were obtained from l5 controls (age, median [range] 47 [23-76] years and 5 patients (MD, -5.7 [-l2.6, +0.7 dB]). During each of 2 sessions, 5 central and 5 peripheral visual field locations were examined on an Octopus 900 perimeter driven by the Open Perimetry Interface (method of constant stimuli, l0 presentations at each of 8 intensities = 800 presentations). Stimulus- response data were fitted with a general linear probit model, separately for each test location (Fig la). Residuals from this model were pooled and investigated as a function of stimulus number (Fig lb).

Original data and results: Nearly all observers showed transient changes in response behaviour over the course of the sessions (see Fig lb for one example). Changes in response latency mirrored those observed in the residuals. Time-series analysis on the pooled data of all observers revealed that drifts occur slowly, over windows of l00 presentations (Fig lc). However, there were no statistically significant relations between the current response and the 5 immediately preceding responses (p=0.68).

Conclusion: While we did not detect significant effects of immediately preceding presentations on responses in a FOS task, many observers showed slow drifts in response behaviour during the test. With the adaptive procedures of clinical perimetry, such changes may be even stronger. Optimising the human-factors aspect of perimetry may help reduce variability in visual fields.

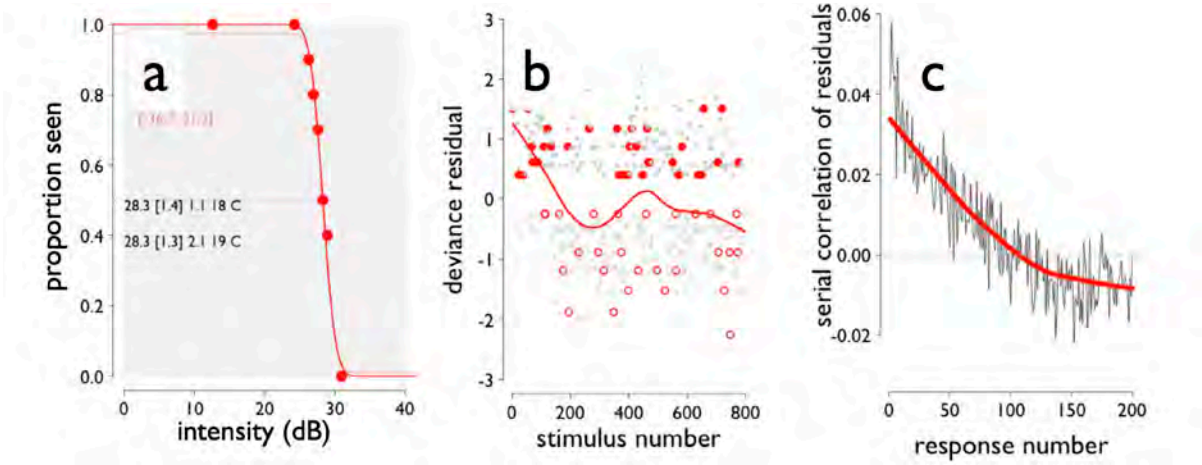

*Fig **1a**) Frequency-of-seeing data from a single test location in the nasal-superior periphery. Ten presentations were made at each of 8 intensities. **b)** Residuals from the entire FOS experiment, plotted in order of presentation. Data from the test location shown in **(a)** are plotted in red. A Lowess fit indicates a substantial drift - the observer responded much more conservatively at the end of the experiment than in the beginning. **c)** Autocorrelation of the residuals, averaged across all observers and sessions. Within a window of approximately 100 presentations, consecutive responses were positively related.*

Acknowledgement: This work was supported by a research grant from the Canadian Clinical Glaucoma Research Council (PHA).

Lateral inhibition in the human visual system in healthy subjects and patients with glaucoma

Authors: *Nomdo M Jansonius, Francisco G Junoy Montolio, Wilma Meems, Marieke SA Janssens, Lucas Stam*
Institutional affiliation: *Ophthalmology, University of Groningen, University Medical Center Groningen, Groningen, the Netherlands*

Design and methodology: The aim of this study was to compare lateral inhibition in the visual system between glaucoma patients and healthy subjects. For this purpose, a case-control study was performed with 14 glaucoma patients and 50 healthy subjects. Cases were selected to have advanced visual field loss in combination with a normal visual acuity. Controls had to have a negative ophthalmic history (except for glasses and uneventful cataract extraction), no family history of glaucoma, an intraocular pressure of 21 mmHg or less, an age between 40 and 70, and a normal visual acuity. Experiments were performed monocularly; the dominant eye was selected if both eyes were eligible. Lateral inhibition was measured psychophysically, with (1) a modified illusory movement experiment (Jansonius and Kuiper 1989) and (2) contrast sensitivity (CS) testing. The tests were presented on a computer screen with a mean luminance of 150 cd/m2. The illusory movement was quantified by nulling it with a real movement; measure of lateral inhibition was the amount of illusory movement. Log CS was measured at 1 and 4 cpd; measure of lateral inhibition was the difference between log CS at 1 and 4 cpd. The amount of illusory movement, log CS at 1 and 4 cpd, and the difference between log CS at 1 and 4 cpd were compared between cases and controls; all analyses were adjusted for age with multiple linear regression.

Original data and results: There was no difference in the amount of illusory movement between cases and controls (P=0.76). Log CS was lower in the cases than in the controls at both 1 (-0.21; P=0.006) and 4 (-0.22; P=0.016) cpd; the difference between log CS at 1 and 4 cpd did not differ between the cases and controls (P=0.84). Lateral inhibition did not depend on age (P=0.93 for illusory movement; P=0.055 for CS).

Conclusion: Lateral inhibition is not decreased in glaucoma patients, at least not in patients with a normal visual acuity. Why is lateral inhibition relevant to glaucoma? In glaucoma, the density of retinal ganglion cells (RGCs) is reduced. It is largely unknown whether and how this influences the spatial interactions between the remaining RGCs. A decrease in lateral inhibition might arise and could result in a larger than expected response to some stimuli, which could mask RGC loss on functional glaucoma testing. A decrease in lateral inhibition may thus play a role in the presumed observation that structural loss precedes functional loss in glaucoma. Our results suggest that this is not the case, and that new tests based on lateral inhibition are unlikely to become very useful in glaucoma.

Psychophysics Paper Session

Temporal summation in early glaucoma: Is the detection of visual field damage a matter of time?

Authors: *Pádraig J. Mulholland,1,2 Tony Redmond,3 David F. Garway--Heath,1 Margarita B. Zlatkova,2 Roger S. Anderson1,2*

Institutional affiliation: 1 National Institute for Health Research (NIHR) Biomedical Research Centre at Moorfields Eye Hospital NHS Foundation Trust and UCL Institute of Ophthalmology, London, UK. 2 Vision Research Laboratory, School of Biomedical Sciences, University of Ulster, Coleraine, UK.
3 Cardiff Centre for Vision Sciences, School of Optometry & Vision Sciences, Cardiff University, Cardiff, Wales, UK.

Background: Standard Automated Perimetry (SAP) is central to the diagnosis and monitoring of visual field damage in glaucoma, but suffers from high measurement variability and only moderate diagnostic sensitivity. Currently, stimulus parameters such as area and duration have been either directly imported from kinetic instruments, or chosen with little regard for changing summation either across the visual field or associated with ocular disease. In this study the effect of varying stimulus duration and area on perimetric thresholds in early glaucoma was examined.

Design and methodology: Twenty patients with open angle glaucoma (mean age: 63 years, mean MD-3.3 dB) and fifteen healthy controls (mean age: 63.6 years) were recruited. Contrast thresholds were collected for a range of stimulus durations (10--200 msec) using both a Goldmann III stimulus (0.48° diameter) and stimuli scaled to the localized area of complete spatial summation (Ricco's area) in four oblique meridians at 8.8° eccentricity in the visual field. All measurements were performed on a high-- resolution achromatic CRT display (frame rate: 121Hz, background luminance: 10 cd/m2). The upper limit of complete temporal summation (critical duration) was estimated using iterative two--phase regression analysis.

Original data and results: Median (IQR) critical duration values were significantly longer ($P < 0.05$) in the glaucoma group for both the Goldmann III equivalent (95.5 msec, 35.5--190.5) and Ricco's area--scaled (93.3 msec, 46.8--162.2) stimuli compared with those of healthy subjects (Goldmann III: 35.5 msec, 15.8-- 43.7; Ricco's area--scaled: 39.8 msec, 23.4-- 64.1). Considering this result in terms of log differences in stimulus energy at threshold, the largest 'glaucoma signal' was observed for stimuli scaled to the localized Ricco's area and shorter than or equal to the critical duration in healthy observers.

Conclusion: Temporal and spatial summation both vary in glaucoma. The duration and area of conventional perimetric stimuli may be inappropriate for identifying early visual field damage. Simultaneously varying stimulus duration, area and luminance during the examination may improve the diagnostic capability of SAP in early disease and also serve to expand the dynamic range of current instruments to more effectively monitor advanced glaucoma.

Poster Session I (3rd Floor)

Moderator: Marta Gonzales-Hernandez

Authors: Fritz Dannheim

Institutional affiliation: Outpatient Eyecare & Orthoptic Unit, 21218 Seevetal, Germany

Design and methodology: We recently found a higher sensitivity of Flicker Perimetry (HEP FDF) for early glaucomatous alterations compared to Standard Automated Perimetry (Octopus SAP), and a higher correlation of HEP visual field- with HRT optic disc parameters [Ophthalmologe 110:131-140 (2013)]. Further follow-up examinations with both perimetric methods include first results with a preliminary release of the Spectralis OCT Glaucoma Module in addition to the HRT.

Original data and results: Perimetric and morphometric results with all 4 techniques are presented for cases with early involvement. The new OCT Glaucoma Module is characterized by its automated localization of the disc margin defined by the inner opening of Bruch's Membrane, topographically connected to the macula. Measurement of the thickness of the retinal nerve fiber layer (RNFL) at the disc margin is no more dependent on the angle of entrance into the disc. Analysis of the RNFL along ring scans of 3 eccentricities further improves the correlation between structure and function. The damage may show up as thinning and /or by vacuoles within the RNFL with corresponding early perimetric changes. The isolated ganglion cell layer provides additional information about early glaucomatous damage.

Conclusion: Both flicker perimetry with the HEP and the new Spectralis OCT Glaucoma Module facilitate early diagnosis in glaucoma.

Poster Session I (3rd Floor)

Comparison of Eye, Head and Shoulder Movements with Respect to Driving Errors

Results of the TUTOR Study

Ulrich Schiefer1,2,3, Elena Papageorgiou1,4, Martin Heister1, Kathrin Aehling1, Christian Heine2, Katrin Sippel5, Thomas Kübler 1,5 Wolfgang Rosenstiel5, Enkelejda Kasneci 5 1 Competence Center Vision Research, University of Applied Sciences, Aalen, Germany 2 Department for Ophthalmology, University of Tuebingen, Germany 3 Research Institute for Ophthalmology, University of Tuebingen, Germany 4 Department for Ophthalmology, University Hospital of Larissa, Greece 5 Computer Engineering Department, University of Tuebingen, Germany

Purpose

To assess the impact of eye, head and shoulder movements as well as driving-related parameters in patients with binocular visual field loss and age- and gender-related ophthalmologically normal subjects on driving performance.

Design and methodology

Forty subjects (10 patients with homonymous visual field defects [H-VFD], 10 patients with binocular glaucomatous visual field loss [G-VFD] and 20 age- and gender-related ophthalmologically normal controls) were enrolled in this project of the TUTOR (TUebingen Traffic Ophthalmology Research) pilot study. They performed an on-road task in a special driving school car with a dual control system – with time-coded recording of eye, head and shoulder movements and other driving-related parameters (such as lane keeping, speed, gap judgement). Statistical analyses comprised one-way ANOVA and paired t test. The significance level was adjusted to an alpha-level of 0.05 for multiple comparisons using TUKEY´s HSD test and BONFERRONI correction, respectively.

Original data and results

Six of ten patients with H-VFD and five of ten patients with G-VFD passed the on-road driving test. In patients with H-VFD or G-VFD who failed the on-road test, head movements ($p < 0.001$), shoulder movements ($p < 0.05$ for H-VFD and $p < 0.001$ for G-VFD, respectively) and lane keeping ($p < 0.05$) were significantly worse compared to age- and gender-related ophthalmologically normal subjects. Visual scanning, driving speed and gap judgement did not show significant differences among the subgroups.

Conclusion

Patients with binocular visual field loss who failed the on-road driving test performed significantly worse with respect to head movements, shoulder movements and lane keeping than age- and gender-related ophthalmologically normal subjects. Head movements were superior to shoulder or eyes movements in predicting the outcome of the driving test.

Literature:
http://www.plosone.org/article/info

Support: MSD, PFIZER, Kerstan Foundation

Title of Abstract: New Options for Early Diagnosis in Glaucoma

Focal relationship between inner retinal layers thickness and macular sensitivity measured with two type of perimetry (standard automated perimetry and microperimetry)

Authors: Shinji Ohkubo1, Sachiko Udagawa1, Tomomi Higashide1, Kazuhisa Sugiyama1, Masanori Hangai2, Makoto Araie 3 , Aiko Iwase4 and Takashi Fujimura 5

Institutional affiliation: Department of Ophthalmology and Visual Science, Kanazawa University Graduate School of Medical Science, Kanazawa, Japan1. Department of Ophthalmology, Saitama Medical University, Saitama, Japan2. Kanto Central Hospital, Tokyo, Japan3. Tajimi Iwase Eye Clinic, Tajimi, Japan4. Topcon Corporation, Tokyo, Japan5.

Design and methodology: Recently increasing attention has been paid to the relationship between structure and function, particularly in the macula. Microperimetry is expected to improve spatial localization. To evaluate the focal relationship between inner macular layer thickness using optical coherence tomography and visual sensitivity measured with standard automated perimetry (SAP) and microperimetry (Macula Integrity Assessment: MAIA) within the central 10° in glaucoma. Forty eyes of 40 subjects with glaucoma were included. The sensitivity of each test point of 10-2 SAP and microperimetry was compared with the corresponding thickness of a 0.5-mm diameter circle containing, ganglion cell layer (GCL), GCL+ inner plexiform layer (IPL) and the retinal nerve fiber layer (RNFL)+GCL+IPL (GCC), with adjusting for retinal ganglion cell (RGC) displacement using Spearman's rank correlation coefficients. Visual sensitivity was evaluated with unlogged 1/Lambert values.

Original data and results: The GCL, (GCL+IPL) and GCC thickness correlated significantly with the sensitivities of 76.4% (rs=0.329-0.735), 76.4% (rs=0.316-0.848) and 95.6% (rs=0.351-0.833) of 68 test points measured with SAP, respectively. In the central 5.8°, the GCL, (GCL+IPL) and GCC thickness correlated significantly with the sensitivities of all test points measured with SAP. The GCL, (GCL+IPL) and GCC thickness correlated significantly with the sensitivities of 72.1% (rs=0.328-0.831), 67.6% (rs=0.320-0.816) and 88.2% (rs=0.331-0.844) of 68 test points measured with microperimetry, respectively.

Conclusion: GCC is the most useful parameter to evaluate structure and function measured with both perimetry within the central 10° in glaucoma. The correlation between structure and function measured with microperimetry were equal with those measured with SAP.

Poster Session I (3rd Floor)

Efficacy of clustered trend analysis for detecting the progression of visual field deficits in glaucoma

Authors: Masahiro Kato, M.D. Tadashi Nakano, M.D., Ph.D. Momoko Kishida M.D. Yoshinori Ito, M.D. Takahiko Noro, M.D. Hiroshi Horiguchi , M.D., Ph.D. Hiroshi Tsuneoka M.D., Ph.D.
Institutional affiliation: Department of Ophthalmology, The Jikei University, School of Medicine,

Design and methodology: A trend analysis using mean deviation slope (MDS) in the Humphrey field analyzer (HFA) is widely accepted to show an advantage of simplicity and feasibility on evaluating progression of visual field deficits in glaucoma. However, the analysis sometimes underestimates the visual field progression, because a local change of visual field tends to be ignored. To compensate such a weak point, the clustered trend analysis has been developed but its clinical utility remains unclear. In the Octopus perimeter, we analyzed the data, which were either directly taken or transferred from HFA, with five sections excised according to the distribution of optic nerve fibers, to evaluate the visual field progression. Then, we compared sensitivity for detecting progression of the deficits between MDS and the clustered trend analysis(CTA).

Patient and methods: Analyses were performed on HFA visual field data, which were collected for a retrospective longitudinal study of patients with glaucoma. The patients were recruited at the glaucoma clinics of the Jikei University Hospital in Tokyo. To evaluate sensitivity for the CTA and MDS, we selected 30 eyes of 20 patients (6 men and 14 women; 60.4 ± 14.3 years old) with HFA data, satisfying the following criteria: 1) measured at least 10 times. 2) P value <0.05 with MDS. The mean number of measurements was 15.5 ± 2.9 times. Data for 26 patients with normal-tension glaucoma and 4 patients with open-angle glaucoma were also included in the analysis. In the CTA, we defined that P value became within it 1% in one or more regions as progression of visual field deficit.

Original data and results: The mean numbers of HFA measurements were 9.5 ± 4.5 times for MDS and 5.8 ± 3.5 times for the CTA; the difference was statistically significant ($P < 0.001$ by t-test). The CTA detected visual field progression in 25 eyes at the earlier timing than MDS. In the other eyes, both methods detected visual field progression at the same timing.

Conclusion: Our data indicate that the CTA detects the progress of visual field deficit more sensitively than MDS.

The relationship between the target speed and reaction time at the location of kinetic threshold

Authors: Tomoyasu Kayazawa1) Chota Matsumoto2) Sachiko Okuyama2) Shigeki Hashimoto2) Hiroki Nomoto2) Fumi Tanabe2) Mariko Eura2) Takuya Numata2) Sayaka Shimada2) Yoshikazu Shimomura2)

Institutional affiliation 1) Department of Ophthalmology, Nara Hospital Kinki University Faculty of Medicine, Nara, Japan 2) Department of Ophthalmology, Kinki University Faculty of Medicine, Osaka-Sayama, Japan

Design and methodology: Kinetic visual field testing has the problem of underestimated visual field area, which is affected by the reaction time (RT). We investigated the relationship between the target speed and RT at the location of kinetic threshold using automated kinetic perimeter. Five normal eyes of 5 normal subjects were tested using an Octopus 900 perimeter with the target size and luminance of III/4e, I/4e, I/3e, I/2e and I/1e and with the target speed from 1 to 10°/sec (total 50 target conditions). The coordinate for average response points (local kinetic threshold; LKT) of 50 target conditions were determined on each meridian of 135° and 225°. Each target was arranged with 1° of the eccentricity farther outside from the coordinate for LKTs and target was presented 1° farther outside each time we obtained the response. The coordinate for the final response points were determined and set as the starting coordinate for RT-vector. RT-vector of all target conditions were presented perpendicularly to each meridian. We examined the relationship between the target speed and RT.

Original data and results: In all target size and luminance, significant difference was observed in the slope of the regression line for the target speed of 1~3°/sec and 4~10°/sec ($p < 0.01$). RT showed a significant negative correlation with target speed of 1~3°/sec ($rs = -0.81 \sim -0.48$, $p < 0.01$) and 4~10°/sec ($rs = -0.69 \sim -0.51$, $p < 0.05$).

Conclusion: The target speed is one of the affecting factors of RT and the difference in the level of RT change by the target speed was seen at the target speed of 3~4°/sec. Correction of LKT using RT needs to use the same level of target speed as was actually used.

Progression Paper Session

More accurate modeling of visual field progression in glaucoma: ANSWERS and structure guided ANSWERS

Authors: Haogang Zhu,1,2 David P Crabb1 and David F Garway-Heath2
Institutional affiliation: 1School of Health Sciences, City University London, UK; 2NIHR BRC at Moorfields Eye Hospital and UCL Institute of Ophthalmology, UK

Design and methodology: Analysis with Non-Stationary Weibull Error Regression and Spatial Enhancement (ANSWERS; Zhu et al, PLoS ONE 2013) estimates the rate of change at locations in the visual field (VF) series, taking into account increasing measurement variability during disease progression and the spatial correlation among test locations. The rate of change may be used to predict future VF sensitivity. ANSWERS can also incorporate structure measures of the retina in a Bayesian framework, leading to structure guided ANSWERS (sANSWERS).

The analysis was undertaken in VF series from the UK glaucoma treatment study (UKGTS; Garway-Heath et al, Ophthalmology 2013), a placebo-controlled trial, in which patients were randomized into latanoprost- and placebo-treated groups and followed up for 2 years. SITA standard 24-2 VFs were acquired with the Humphrey Field Analyser (Carl Zeiss Meditec, CA) and the optic disc rim areas were acquired with Heidelberg Retina Tomograph (Heidelberg Engineering, Germany). Only the VFs with false positive response <15% were used, resulting in 659 eligible eyes of 437 patients. ANSWERS and ordinary least squares linear regression (OLSLR) were used to predict the VF at next visit using subseries that are within 7, 13, 18 or 22 months from the baseline visit. The prediction accuracy was summarized by the mean normalized squared error (MNSE): which is the squared prediction error in percentage with regard to the measurement variance at the 52 individual locations in VF. The prediction accuracy of ANSWERS in comparison with OLSLR was made. In a preliminary analysis of a subset of 143 subjects, the rate of change in log rim area was incorporated into sANSWERS as the prior probability. The difference in the rates of change in VF loss by ANSWERS and sANSWERS (with the structural prior) was compared in the latanoprost and placebo groups.

Original data and results: With all lengths of subseries, ANSWERS produces significantly (<0.01%, Wilcoxon signed rank test) more accurate prediction than OLSLR. The average MNSE of ANSWERS is 11% lower than that of OLSLR. In particular, the prediction accuracy of ANSWERS is better in shorter series, with the MNSE (median [95% confidence interval]) of ANSWERS being 38% [34%, 41%] lower than that of OLSLR in subseries of 7 months from baseline. The difference in the rate of VF change between the latanoprost and placebo groups with sANSWERS has greater significance (P = 5%) than that from ANSWERS (P = 9%).

Conclusion: ANSWERS predicts future VF loss better than OLSLR across a wide range of series lengths, but especially with short series. The rate of VF change from sANSWERS better separates the latanoprost and placebo groups, suggesting greater accuracy and precision of estimates of VF loss by incorporating a structural prior.

Visual field Assessment in the Idiopathic Intracranial Hypertension Treatment Trial using Pointwise Linear Regression

Authors: Michael Wall, Colleen M. Kummet, Gideon Zamba, Chris A. Johnson, Kimberly E. Cello, John L. Keltner and Michael P. McDermott for the NORDIC IIH Study Group

Institutional affiliation: University of Iowa, UC Davis KEC, JLK, University of Rochester MPM

Design and methodology: The Idiopathic Intracranial Hypertension Treatment Trial (IIHTT) is a multicenter, double-blind, randomized clinical trial comparing acetazolamide and placebo on visual outcome. Our aim was to determine visual field change over time using pointwise linear regression. We enrolled 165 IIH subjects, with a mean deviation between -2 dB and -7 dB in the most affected eye (study eye) who received a weight reduction diet plus acetazolamide or diet-plus-placebo and followed patients with perimetry for six months. Subjects were tested twice at baseline and six months, We used pointwise linear regression to classify locations within the eye as improving using the criteria 1) any positive slope and 2) positive slope outside of the 95% CI for the mean of 26 healthy observers for that location. The study eye and fellow eye were classified separately.

Original data and results: < Over 60% of study eyes (74 of 121 subjects with complete data) showed significant positive slope ($p<0.05$) in threshold sensitivities for at least 2 locations within the visual field. Across subjects, an average of 36 of 52 locations in study eyes had improving sensitivities over time. When compared to healthy observers, 37 locations in study eyes on average were greater than the mean of control sensitivities within the same location. Negative slopes over time were observed in about 15 locations on average for study eyes.
The Figure shows the percentage of positive slopes by location – note that the improvements occurred across the central visual field with a range of only about 10%.>

Conclusion: Significant positive trends in pointwise threshold sensitivities were observed over time for the majority of study participants. The changes appeared to be mostly generalized across the central visual field rather than localized. This has important implications on how to follow idiopathic intracranial hypertension patients; the mean deviation may be the appropriate measure.

Percent of Subjects with Positive Slope in each Location

			70.2%	72.7%	72.7%	71.9%	
		71.1%	72.7%	71.1%	66.9%	71.1%	66.1%
	72.7%	73.6%	63.6%	71.1%	66.9%	68.6%	72.7%	72.7%
75.2%	75.2%	75.2%	71.9%	73.6%	63.6%	62.8%		68.6%
69.4%	68.6%	71.1%	70.2%	64.5%	67.8%	72.7%		76.0%
	65.3%	68.6%	65.3%	63.6%	67.8%	71.9%	72.7%	70.2%
		67.8%	66.1%	65.3%	71.1%	71.9%	74.4%	
			66.1%	67.8%	68.6%	73.6%		

Progression Paper Session

Global Visit Effects in Pointwise Longitudinal Modeling of Glaucomatous Visual Fields

Authors: S.R. Bryan1,2, K.A. Vermeer1, E.M.E.H Lesaffre2,3, H.G. Lemij4 and P.H.C. Eilers2

Institutional affiliation 1. Rotterdam Ophthalmic Institute, Rotterdam, The Netherlands; 2. Department of Biostatistics, Erasmus Medical Center, Rotterdam, The Netherlands; 3. KU Leuven, L-Biostat, Leuven, Belgium; 4. Glaucoma Service, Rotterdam Eye Hospital, Rotterdam, The Netherlands

Design and methodology: Evaluation of a longitudinal series of visual fields (VF) provides a means to detect glaucoma and to determine functional deterioration. One of the difficulties in modeling VF data is the sometimes large and correlated measurement errors in the pointwise sensitivity estimates. This may be due to measurable factors, such as season, time of day and reliability indices, or unknown transient factors, such as fatigue, lack of concentration, or delayed reaction time. As these factors affect all locations belonging to the same visual field, we propose to model them as Global Visit Effects (GVE). VFs (24-2 Full Threshold) of 50 patients from The Rotterdam Eye Hospital with primary glaucoma were included in the analysis (data available at http://orgids.com). Sensitivity estimates in 52 locations in both eyes were included in a hierarchical Bayesian mixed effects model with four levels: individual, eye, hemisphere and location. Censoring was taken into account at 0 dB. The contribution of the GVE was evaluated by comparing the observed data and the posterior predicted values for the models with and without this effect (see Figure 1). Furthermore, the importance of the GVE was determined by comparing the magnitude of this effect to known factors. Finally, the GVE's effect on the estimated slopes was evaluated by determining the absolute difference between the slopes with and without the GVE.

Original data and results: Including the GVE showed a highly significant improvement in the model fit, reducing the mean absolute error from 2.14 dB to 1.94 dB. In addition, the magnitude of the GVE (0.82 dB) was much larger than any of the other known factors, namely season (0.07 dB), time of day (0.14 dB), percentage of fixation losses (0.09 dB), percentage of false positives (0.09 dB) and percentage of false negatives (0.07 dB) and more than 3 times larger than those factors combined (0.25 dB). The average absolute difference in slopes with and without the GVE was 0.08 dB/year.

Conclusion: Including an overall visit effect showed a highly significant improvement in the model fit. The GVE's magnitude is far larger than other factors and affects the estimated slope. By lowering the residual error, better estimates of the real evolution of the sensitivity over time may be obtained.

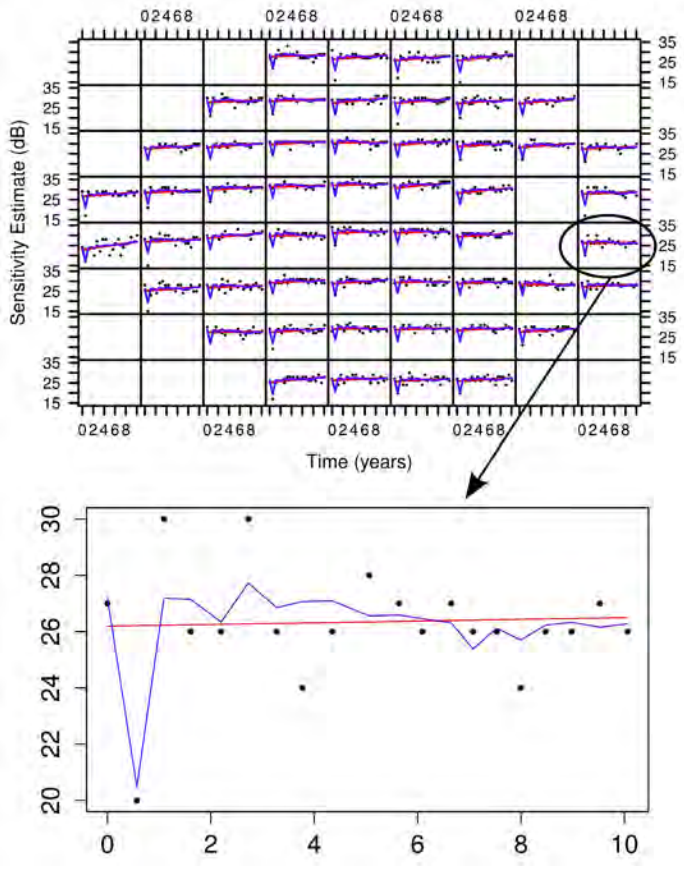

Figure 1 The scatter plot represents the retinal sensitivity estimates over time for each location of the VF in an example (right) eye. The lines represent the model fits with (blue) and without (red) the visit effect.

Improved prediction accuracy using the most recent visits within a longitudinal follow-up test series with the dynamic structure-function model

Authors: Rongrong Hu,1,2 Iván Marín-Franch,3 Lyne Racette1
Institutional affiliations: 1Indiana University, Eugene and Marilyn Glick Eye Institute, Indianapolis, USA; 2Department of Ophthalmology, First Affiliated Hospital, College of Medicine, Zhejiang University, Hangzhou, China; 3Grupo de Investigación en Optometría (GIO), Universitat de València, Burjassot, Spain

Design and methodology: The dynamic structure-function (DSF) model quantifies structural and functional changes over time and uses two descriptors, a centroid and its velocity vector. The centroid estimates the current state of the disease and the velocity vector estimates the direction and rate of change over time. Based on the latest centroid and velocity vector, the expected observations at the next visit can be predicted. We previously reported improved prediction accuracy for the DSF model compared to ordinary least squares linear regression (OLSLR) when short follow-up series are available (three to six visits). The purpose of the present study is to determine whether the prediction accuracy of the DSF model can be improved by using the most recently available tests from a longitudinal series compared to the entire follow-up series. We used longitudinal data of paired rim area (RA) and mean sensitivity (MS) from 220 eyes with ocular hypertension or primary open-angle glaucoma enrolled in the Diagnostic Innovations in Glaucoma Study or the African Descent and Glaucoma Evaluation Study. RA and MS were expressed as percent of mean normal based on an independent dataset of 91 healthy eyes. Each eye had 11 longitudinal data pairs (visits). Series of different length were used to predict the 11th visit: visits 7 to 10 (referred to as Series 4) were used to predict visit 11, visits 6 to 10 (Series 5) were used to predict visit 11, and so on until visits 1 to 10 (Series 10) were used to predict visit 11. We compared the prediction error (PE) obtained with the DSF model using the different series. We also compared the PE obtained with the DSF to that obtained with the OLSLR. We used the Wilcoxon signed-rank test to test significant differences at a level of 0.05.

Original data and results: Using the DSF model, the median PE were 10.80, 10.28, 10.76, 10.73, 10.42, 11.40 and 11.42 percent normal for Series 4 to 10, respectively. The lowest PE was for Series 5 and was significantly lower than that of Series 10 ($p = 0.02$). Using the OLSLR, the median PE were 13.87, 13.44, 12.61, 12.02, 11.55, 11.59, and 11.22 percent normal for Series 4 to 10, respectively. The PE of the DSF model using Series 5, 6, and 7 were significantly lower than those for the OLSLR using Series 8, 9, and 10 (all p-values < 0.05).

Conclusion: Prediction accuracy of the DSF model improved when the most recent tests in a series were used. Our results suggest that more accurate predictions can be made with the DSF model using a smaller number of recent visits compared to OLSLR. This may be useful clinically, where early detection of glaucoma progression is crucial for patient care.

Progression Paper Session

Comparisons of robust linear regression and simple linear regression models in predicting visual field progression

Authors: Yukako Taketani M.D., Hiroshi Murata M.D., Ryo Asaoka M.D. Ph.D.
Institutional affiliation : Ophthalmology department, Graduate School of Medicine, The University of Tokyo

Design and methodology:
Using various numbers of prior visual fields (VF, minimum 1st-5th: VF1-5 and maximum 1st-14th: VF1-14), point-wise sensitivities of 1st (approximately 7 months later), 2nd (approximately 17 months later) and 3rd (approximately 25 months later) future VFs (HFA 30-2 SITA-standard) were predicted by applying simple linear regression. Similar procedures were performed using M-estimator robust linear regression and deepest linear regression.

Original data and results:
Subjects comprised of 44 open angle glaucoma patients with 15 VFs spanning on approximately 9 (sd: 1.3) years. Unreliable VFs, defined as having more than 20% fixation losses and more than 15% false positive errors, were excluded beforehand. In the simple regression model, minimum absolute prediction error was obtained with VF1-13 (2.7±0.7 dB), VF1-11 (3.0±1.1 dB) and VF1-11th (3.4±1.0 dB) when predicting 1st, 2nd, 3rd future VF, respectively. The mean of the absolute prediction error reached within 95% confidence interval (CI) of the minimum absolute prediction error using VF1-9 (for 1st future VF), VF1-7 (for 2nd future VF) and VF1-10 (for 3rd future VF). Smaller minimum absolute prediction errors were obtained with the M-estimator robust and deepest linear regressions with the improving rates ranging from 4 to 8 %. With these robust regression models, at least VF1-7 or VF1-8 were needed to reach the within 95% CI of the minimum absolute prediction error with the simple regression.

Conclusion:
These results suggest considerable numbers of VFs are needed to achieve accurate prediction of the VF progression, with the simple linear regression. Smaller prediction errors were obtained with the robust regression models with slightly smaller numbers of VFs than the simple regression model.

Using eye movement scanpaths recorded during free viewing of movies to detect vision loss in glaucoma: a proof of principle study

Authors: Nicholas D. Smith, Haogang Zhu, David P. Crabb
Institutional affiliation: Division of Optometry and Visual Science, City University London.

Design and methodology: Typical vision tests require people to perform the unnatural task of maintaining steady fixation whilst responding to synthetic stimuli. In this exploratory study we test the hypothesis that vision loss in glaucoma can be detected by examining patterns of eye movements recorded whilst a person naturally watches a movie. Thirty-two people with normal vision (median age: 70, interquartile range [IQR] 64 to 75 years) and 44 patients of a similar age with a clinical diagnosis of glaucoma (median age: 69, IQR 63 to 77 years) had standard vision examinations including automated perimetry. All participants then viewed three unmodified TV and film clips whilst their eye movements were monitored using an Eyelink 1000 eyetracker (SR Research, Ontario, Canada). Scanpaths were then plotted using purpose-written software that first filtered the data and then generated saccade density maps. This procedure involved a centralization process, whereby each saccade made by a participant during the videos was treated as a vector starting at [0,0]. The proportion of saccades that ended in each region of the visual field could then be calculated. The resulting saccade density maps were then subjected to a feature extraction analysis using kernel principal component analysis (KPCA) and classified using a naïve Bayes classifier. The classification was trained and tested by a 10 fold cross validation which was repeated 100 times to estimate the confidence interval (CI) of classification hit rate and specificity.

Original data and results: Patients had a range of glaucoma disease severity (median worse eye MD of -11.7 dB, IQR -17.1 to -5.9 dB). Average hit rate for correctly identifying a glaucoma patient at a fixed specificity of ~90% was 79% (95% CI: 67 to 93%). The area under the Receiver Operating Characteristic curve was 0.84 (95% CI: 0.79 to 0.92).

Conclusion: Huge data from scanpaths of eye movements recorded whilst people naturally watch videos can be processed into maps that contain a signature of vision loss. This proof of principle study demonstrates that a group of patients with a range of glaucomatous vision loss can be reasonably well separated from a group of peers with normal vision by considering these eye movement signatures alone. Estimates of 'diagnostic precision' for this approach are similar to what would be found using a single result from a modern imaging device.
This work was kindly supported by Fight for Sight.

Novel Approaches Paper Session

Multifocal stimuli presented in spatially-clustered volleys increase SNRs in pupil perimetry.

Authors: CF Carle1, AC James1, M Kolic1, RW Essex1,2, T Maddess1
Institutional affiliation: 1John Curtin School of Medical Research, The Australian National University, Canberra, Australia.
2 Dept Ophthalmology, The Canberra Hospital, Canberra, Australia.

Design and methodology: Signal to noise ratios (SNRs) of a novel multifocal pupillographic objective perimetry (mfPOP) method in which stimuli are presented in clustered volleys (CV) were compared with those obtained using our original spatially-sparse presentation. Results encompassing 5 studies and 398 mfPOP fields are summarized. Seventy three subjects with normal vision (37 males) were included, having been tested in these studies using otherwise-identical mfPOP variants i.e. stimuli presented using either the spatially-sparse or CV methods. MfPOP variants with 30 or 60 degree fields and a range of luminance levels were assessed. Pupillary sensitivities at 44 regions per field were measured, and expressed as z-score SNRs.

Original data and results: Subject ages were distributed uniformly with the mean ages (± SD) of subjects in each of the five studies ranging from 21.0 ± 1.0 y to 70.2 ± 4.9 y. The mean z-score and SE for CV presentation across studies was 4.37 ± 0.23SD, 40% ± 11%SD higher than spatially-sparse presentation. This increase was significant in all 5 studies at $p < 0.005$ (Table 1).

Table 1. Summary of 5 studies examining the percent increase in SNR using clustered volley presentation (CV) instead of spatially-sparse. ***p* <** indicates the significance of the % increase.

Study	Study type	mfPOP variants tested†	*n* subjects (males)	Ages y ± SD	Z Achieved mean ± SE	SNR % increase	*p* <
SNR1	Normals	Y_{wide}, 2 repeats	6 (3)	38.2 ± 19	**4.47** ± 0.27	**60%**	10^{-6}
SNR2	Normals	Y_{wide}, 2 repeats, 4 luminance levels	6 (3)	37.7 ± 20	**4.36** ± 0.31	**29%**	0.005
PreG	Normal/ glaucoma	Y_{wide}, 2 repeats	24 (12)*	66.0 ± 8.6	**4.30** ± 0.19	**34%**	10^{-5}
SNR4	Normals	$Y_{macular}$, 4 luminance levels	18 (9)	21.0 ± 1.0	**4.13** ± 0.17	**39%**	0.001
PreA	Normal/ AMD	$Y_{macular}$	19 (8)*	70.2 ± 4.9	**4.60** ± 0.21	**38%**	10^{-8}

* refers to the normal subjects included in this analysis only and is exclusive of patients
† Y = yellow stimuli on yellow background. $_{wide}$ refers to 60° field, $_{macular}$ to 30°

Conclusion: Objective perimetry has been limited by relatively low SNRs. This means that long test durations are needed to achieve clinically relevant sensitivity, specificity and reproducibility. CV presentation improved mfPOP SNRs by an average of 40%; to achieve this result using spatially-sparse presentation would require test durations of 11.7 min compared to the 6 min to test both eyes used here. As well as the potential for improved measurement accuracy, this increase in SNR opens up a number of possibilities such as even shorter test-durations or greater flexibility in stimulus parameters.

Assessment of anterior lamina cribrosa surface depth in glaucoma and healthy eyes.

Authors: Akram Belghith1, Christopher Bowd1, Zhiyong Yang1, Ting Liu1, Felipe A. Medeiros1, Robert N. Weinreb1, and Linda M. Zangwill1.
Institutional affiliation: 1Ophthalmology, Hamilton Glaucoma Center, University of California San Diego, CA, USA

Design and methodology: The purpose of this study was to evaluate the ability of anterior lamina cribrosa surface (ALCS) measurements for discriminating between healthy and glaucoma eyes. We propose a new approach for the segmentation of the Bruch's membrane (BM) layer and the ALCS to measure the ALCS depth from 3D Spectralis SD-OCT images (Heidelberg Engineering, 48 enhanced depth imaging EDI radial B-scans centered on the optic nerve head). The delineation of these structures is addressed using a Bayesian framework where the different priors we have were injected in the inference scheme. The locations of the Bruch's membrane opening (the termination of the Bruch's membrane layer) for each radial scan are then estimated using an artificial neural network principal component analysis procedure (ANN-PCA) to model the elliptical shape of the 3D BMO points. The ALCS depth (ALCSD) parameter was generated as the average perpendicular distance from ALCS relative to the BMO reference plane along 24 radial scans. Two experts manually marked the border of the ALCS at 8 predefined locations on every radial scan. We compared the ALCSD measurements using the proposed framework to those obtained by expert manual segmentations. Glaucoma diagnostic accuracy (area under receiver operating characteristic (AUROC)) was then estimated for the proposed method and for expert segmentation.

Original data and results: Measurements were obtained from 50 eyes of 25 glaucoma patients (61.32 ± 8.94 years) with mean deviation (MD) values ranging from 1.728 to -14.94 dB and 50 eyes of 30 normal subjects (58.17 ± 7.53 years). Study participants were recruited from the Diagnostic Innovations in Glaucoma Study (DIGS). The correlations were: between the two experts R2 = 0.91 ($p < 0.001$), between expert 1 and the automated method, R2 = 0.94 ($p < 0.001$) and between expert 2 and the automated method, R2 = 0.925 ($p < 0.001$). The percentages of difference <10 pixels were: 74% for expert1 and expert2, 84% for expert1 and the automated method and 80% for expert 2 and the automated method. The AUROC (95%CI) for discriminating between glaucoma and normal eyes was 0.54 (0.41-0.64) for expert1, 0.57 (0.48-0.7) for expert2 and 0.65 (0.53-0.77) for the automated method.

Conclusion: Only classification by automated ALCSD delineation performed better than chance at separating glaucomatous from healthy eyes. Agreement between our automated method and subjective expert assessment was similar to that between the 2 experts. ALCSD measurement holds promise for objectively classifying eyes as glaucomatous.

Novel Approaches Paper Session

Investigating the impact of visual field defect location on the detection of driving hazards

Authors: Fiona C. Glen, Nicholas D. Smith & David P. Crabb.
Institutional affiliation: Division of Optometry and Visual Science, City University London.

Design and methodology: Binocular visual field (VF) loss is linked to an increased likelihood of motor accidents. Driving authorities therefore require patients to surrender their license if their VF defect is deemed to have reached an 'unsafe' level. Yet, evidence is surprisingly limited regarding the specific types of VF defect that impair driving performance. This study employed a novel gaze-contingent display to test the hypothesis that location of VF loss impacts performance on the driving Hazard Perception Test (HPT). The HPT is a required component of the UK driving exam for learner drivers. The computer-based test requires participants to respond to hazardous events within 14 real-life driving films, with overall performance scored out of 75 depending on how efficiently they respond to 15 test hazards. Thirty UK drivers with healthy vision completed three versions of this test in a random order. In two versions, a bespoke computer set-up incorporating an eye-tracker modified the position of an image distortion that coincided with the simulated position of a VF defect; this was done in the superior and inferior VF respectively according to the user's real-time gaze as they completed the assessment. Everyone also completed an unmodified version of the HPT as a measure of their baseline performance. A repeated-measures ANOVA was used to investigate within-person differences in performance. Participants also completed a short assessment of higher-order visual processing abilities relevant to driving ("Trail B assessment") to determine whether any changes in performance were linked to a slower general visual processing speed. This study was approved by a Research and Ethics committee at City University London.

Original data and results: Participants scored 49 out of 75 on average (standard deviation [SD]=9) when completing the unmodified version of the HPT. Mean (SD) performance fell by 18% [40(11)] when viewing films with a superior defect, and 12% with an inferior defect [43(10)]. A repeated-measures ANOVA tested within-person differences in performance and the main effect was significant ($p<0.001$). Pairwise comparisons showed performance was significantly worse with a superior defect compared to an inferior defect ($p=0.01$; 95% CI for mean difference=1 to 7). A slower processing speed in the Trail B assessment was not related to heightened task impairment relative to baseline when completing the task with either defect (rho=0.05 and -0.07 respectively).

Conclusion: In this study, simulated VF defects impaired ability to detect driving hazards relative to participants' normal performances. Furthermore, the location of VF loss was important: we found superior VF defects were more 'hazardous' than inferior defects. This study could help inform the design of fairer tests and standards for the VF component for fitness to drive.

This study was supported by a research award from the International Glaucoma Association.

A comparative analysis of changes in visual field sensitivity in type 2 diabetes

Authors: Faran Sabeti, Rakesh Mallikarjunan, Christopher Nolan, Corinne Carle, Ted Maddess, Andrew James
Institutional affiliation Australian National University

Design and methodology: The aim of the study was to investigate the effect of diabetic retinopathy (DR) severity on multifocal pupillographic objective perimetry (mfPOP) compared with Humphrey Matrix and short wavelength automated perimetry (SWAP). Seventy eyes of 35 subjects with type 2 diabetes, with no to minimal (sev1, n=40), and moderate to severe (sev2) DR (n=30) based on ETDRS fundus photos, and 20 age and sex-matched control subjects were recruited from The Canberra Hospital. At visit one participants were randomly tested with a Macularfield (±15° eccentricity from fixation) and Widefield (±30° eccentricity) mfPOP stimulus protocols and Humphrey Matrix perimetry. At visit 2 the mfPOP protocols were repeated, followed by SWAP. MfPOP stimulus protocols utilized yellow luminance-balanced stimuli with a peak luminance of 150 and 288 cd/m2 for the Widefield and Macularfield protocols respectively. Stimuli were presented for 33 ms duration at a mean interval of 4 s to each of the 44 visual field regions in a clustered volley presentation method. Visual sensitivity were calculated globally and for four eccentricities (3°, 9°, 15° and 21°) for Matrix and SWAP perimetry and five eccentricities (4°, 8°, 12°, 18° and 24°) for mfPOP. Generalised mixed models were used to determine the effect of retinopathy severity on visual field sensitivity.

Original data and results: The mean effect of disease on Matrix mean deviation (MD) showed a significant reduction in sensitivity of -1.77 dB ± 0.82 for sev1; and -2.33 dB ± 1.07 for sev2 patients respectively compared with controls: 1.25 dB ± 0.57 (mean effect ± SE, all $p<0.05$). SWAP MDs were significantly reduced only for sev2: -1.80 dB ± 0.82 compared with controls: 0.11 dB ± 0.57 (both $p<0.05$). However, pattern standard deviations (PSDs) were significantly increased for both sev1 and sev2 for SWAP: 1.5 dB ± 0.21; and 1.8 dB ± 0.23 (both $p<0.05$). The effect of disease on Matrix PSD did not reach significance. MD did not differ between sev1 and sev2 for Matrix or SWAP. Ring-wise means showed significant reduction in sensitivity with increasing eccentricity for both sev1 and sev2 groups with the largest deviation in the outermost ring (-6.97 dB ± 1.4, $p<0.0005$; -2.57 dB ± 1.18, $p<0.05$ for SWAP and Matrix respectively). On average, the effect of sev1 and sev2 DR on mfPOP mean deviation did not reach significance for either the Macularfield or Widefield protocols. However, ring wise analysis showed that relative to the central ring in controls, amplitude deviations were significantly reduced across most rings for sev2 group with the largest deviation presenting in the outermost ring (-0.23 dB ± 0.09, $p<0.05$) in the Widefield stimulus protocol. Mean ring wise effects for sev3 did not reach significance due to larger than normal responses. Time to peak mfPOP responses were significantly delayed across all rings in sev3 but not in sev2 (both $p<0.05$).

Conclusion: Matrix perimetry and mfPOP may be more sensitive to visual field loss than SWAP in type 2 diabetic patients with minimal to no signs of DR (n=40). MfPOP had the advantage of identifying a changing dominance between amplitude and delay with disease progression. Further investigation of prognostic biomarkers in mfPOP identifying eyes at risk of retinopathy progression is warranted.

Novel Approaches Paper Session

Retinal displacement and M-CHARTS score in simulated metamorphopsia

Authors: C Matsumoto1, E Arimura-Koike 2, H Nomoto, M Eura1, S Okuyama1, S Hashimoto1, F Tanabe1, S Shimada1, Y Shimomura1
Institutional affiliation: 1Department of Ophthalmology, Kinki University Faculty of Medicine, Osaka-Sayama, Japan, 2Department of Ophthalmology, Sakai Hospital Kinki University Faculty of Medicine, Sakai, Japan

Design and methodology: Metamorphopsia is one of the common symptoms in several macular diseases. The main cause of the metamorphopsia is suspected to be the disarray of the photoreceptors in the sensory retina. Using M-CHARTS developed by us, we estimated the relationship between the degree of retinal displacement and M-CHARTS score in the simulated metamorphopsia and epiretinal membrane (ERM) subjects. Using M-CHARTS, we generated the artificial target displacement and measured the detectability of the distortion in 20 normal volunteers. We also evaluated the M-CHARTS scores in 29 eyes of 29 ERM patients observed for at least 3 years. Horizontal and vertical retinal contraction due to ERM was measured by the locations of retinal vessels on sequential fundus images.

Original data and results: In the simulated metamorphopsia, M-CHARTS score 0.4 was equivalent to 0.016, 0.019, 0.021 and 0.025mm retinal displacement at 2, 4, 6 and 8 degree eccentricity from the fovea, respectively. M-CHARTS score 1.0 was equivalent to 0.023, 0.039, 0.043 and 0.055 mm retinal displacement at 2, 4, 6 and 8 degree eccentricity, respectively. In ERM subjects, when vertical M-CHARTS score increased to 0.4, horizontal 0.06mm retinal contraction was observed. When the horizontal M-CHARTS score increased 0.4, vertical 0.065 mm retinal contraction was observed. The retinal displacement in ERM was relatively larger than theoretical simulation results.

Conclusion: Metamorphopsia score using M-CHARTS was correlated with the degree of the anatomical retinal displacement.

A new game-based visual field test for paediatric use.

Authors: Marco A. Miranda,1,3 David B. Henson,1,2 Cecilia Fenerty,1,2 Susmito Biswas,2 Tariq Aslam1,2
Institutional affiliation 1. Faculty of Medical and Human Sciences, Institute of Human Development, The University of Manchester, Manchester, UK; 2. Royal Eye Hospital, NHS Central Manchester University Hospitals, Manchester, UK; 3. NIHR Biomedical Research Centre, Moorfields Eye Hospital and UCL Institute of Ophthalmology, London, UK.

Design and methodology: Aim: To extend the development of a novel concept for paediatric visual field (VF) testing based on a computer game where software and hardware combine to provide an enjoyable test experience.

Methods: The test software was developed in MatLab-2014A using Psychtoolbox-3.0 (PTB). It consists of a platform-based computer game shown on the central VF. A storyline was created around the game as was a structure surrounding the computer monitor to enhance patients' experience. The patient is asked to help the central character, a prince with a curse which transformed him into a frog, collect magic coins (stimulus) which give him powers to reverse the curse. To collect these magic coins, series of obstacles need to be overcome. The test was presented on a Sony PVM-2541A organic LED monitor, which was calibrated from a central midpoint with a photometer, Minolta CS-100, placed at 50cm. Measurements were performed at 15 different locations on the screen and the contrast calculated based on the Humphrey Field Analyser. An Optical Transient Recorder (OTR-3) was used to compare PTB self-reported and the actual stimulus duration. Stimuli were chosen from a scale ranging from 0.046 to 2.441 degrees subtended (factor: 1.19). Differences between the intended and presented stimuli sizes, error, were calculated. To test the feasibility of the novel approach 14 patients (4-11 years old) with no history of VF defects were recruited. The study was approved by the North West Lancaster Research Ethics Committee. Unless stated otherwise, data is presented as mean ± standard deviation of the mean.

Original data and results: For the 8 subjects completing the study (4 withdrew for reasons external to the project and 2 due to malfunction of the head-rest sensor or test software) 31±20 data points were collected on 1 eye of each patient on 4 different peripheral and central locations of the field. Background luminance ranged between 9.19 to 10.4cd/m2 and stimulus contrast between 27.7 and 28.2dB. No difference was found between measured and self-reported stimulus duration. Stimuli size errors subtended 0.0196±0.0079 degrees and were presented every 13.8±17.7sec for 211.6±7.8msec (PTB self-reported).

Conclusion: Preliminary data shows the feasibility of a game-based visual field test for paediatric use. Although the test time was longer than usual due to the game nature of the test, it was well accepted by the target population. Background and stimuli luminance uniformity varied little across the screen. Stimuli durations similar to those of the clinical gold-standard test were achieved.

Figure: Top left: Image of the central character of the game before being cursed by a witch. Top Right and Bottom Left: Images of the central character transformed into a frog and obstacles to overcome. Bottom Right: Apparatus for the Crazy Castle. The OLED monitor is situated inside the Castle.

Acknowledgement: This abstract presents independent research funded by the National Institute for Health Research (NIHR) under its Research for Patient Benefit (RfPB) Programme (Grant Reference Number PB-PG-0211-24064). The views expressed are those of the author(s) and not necessarily those of the NHS, the NIHR or the Department of Health.

Poster Session II (3rd Floor)

Moderator: Paul H. Artes
Assessment of visual impairment from binocular visual field defects

Authors: Fritz Dannheim, MD1, Dagmar Verlohr, Orthoptist1, 2
Institutional affiliation: 1Outpatient Eyecare & Orthoptic Unit, 21218 Seevetal, GER,
2Centre for Neurological Therapy, 21266 Jesteburg, GER

Design and methodology: Binocular defects in the central visual field can cause deficits in orientation and reading, leading to loss of quality of life, e.g. by increased risk of falling or limited participation in various activities including occupation and traffic. In 2004 we presented a test for visual performance in cerebral lesions at the IPS Symposium [www.perimetry.org/meetings/IPSAbstractBooks]. Now, after more than 10 years of experience, we can offer a professional software version "VisioPercept®", a test for measuring visual reaction and asymmetry. The time required for detecting "Lea Numbers®" in free gaze, appearing on a scenic PC screen in 11 positions within 34° in random order, is recorded for 2 sequences. Indices like short term fluctuation and asymmetry within the hemispheres as well as reliability of correct recognition of the numbers are printed underneath the topographic result. Cases with spontaneous adaptation to their deficit by compensatory search saccades may be separated from those who require rehabilitation training. The effect of training can be verified by follow-up tests.

Original data and results: In 52 patients we found a normal visual competence in spite of homonymous defects, 31 of them were motivated to drive again. A retrospective interview revealed that 7 had successfully passed an on-road driving exam, 2 a specific traffic test for visually handicapped. In one case the permission was denied due to minor mistakes. Twelve patients were driving again without official permission. Problems with driving did not show up in any of these cases. Our actual checklist contains a sequence of expert's reports by an Ophthalmologist, a Neuropsychologist and a specific driving examiner, before the patient can apply for an individual driving permission. Traffic authorities in our region in Germany have generally no objections.

Conclusion: Patients with binocular visual field defects may reach a normal level of visual competence, thus regaining high quality of life and independency.

Switching to stimulus size 5: are the results compatible with standard stimulus

Authors: Joerg Weber
Institutional affiliation: Augenarztpraxis Koeln

Design and methodology: It is well accepted that stimulus size 5 has several advantages compared with size 3: Less influence of correcting glass errors, optic abnormalities and cataract, larger dynamic measurement range. The lack of normal data for size 5 was an obstacle for routine clinical use. As this data is now available, we examined the question whether norm related data (total deviation or defect depth, index MD) is comparable and we can switch from size 3 to size 5 during follow up.
15 Glaucoma patients and 8 normals were examined with standard automated perimetry on the HFA using size 3 and size 5. We compared the MD and the pattern of the defect.

Original data and results: The MD Differences ranged from +1,3dB to -2.1dB. The average difference was -0.3 dB. In the cases with field defects, neither size nor defect depth (when the higher measurement range was cutoff) showed considerable mismatch. Most of the patients preferred the size 5 examination.

Conclusion: In patients with advanced glaucoma defects, it is possible to switch to the stimulus size 5 without a break in follow-up. This will give a larger measurement range. Also patients with optic problems as irregular astigmatism may profit from a change of the method. Last but not least, patients complaining about the "very small white points" may be happier with the larger stimuli.

Poster Session II (3rd Floor)

Monitoring vigilance during automated static perimetry

Matthias Müller1, Judith Ungewiss1*, Enkelejda Kasneci2, Wolfgang Rosenstiel2, Ulrich Schiefer1,3,4*
1 Competence Center Vision Research, University of Applied Sciences, Aalen, Germany
2 Computer Engineering Department, University of Tuebingen, Germany
3 Department for Ophthalmology, University of Tuebingen, Germany
*4 Research Institute for Ophthalmology, University of Tuebingen, Germany *equally contributed*

Purpose
To monitor subjects' vigilance by means of infrared (IR)-pupillography during automated static visual field assessment in a conventional, commercially available perimeter.

Design and methodology
MoCS (Method of Constant Stimuli) was used to assess differential luminance sensitivity within the central 30° visual field with the OCTOPUS 900 perimeter (Haag-Streit AG, Koeniz, Switzerland) using OPI (Open Perimetry Interface). Thus, in contrast to Henson (2010), a commercially available bowl perimeter was used. Stimulus intensity was varied in six steps between 0.50 and 20.08 cd/m2 with constant background luminance of 10 cd/m2. Each stimulus intensity level was repeated 30 times in randomized order at three locations: (0°/0°), (-5°/-5°), (+5°/+5°). False-positive and false-negative catch trials were implemented (5% each). The subjects were instructed to fixate a central diamond and to press a response button in case of stimulus perception. Pupil diameter was extracted from the IR camera monitoring the fixation. The occurrence of fatigue was detected by using GNU R applying a wavelet transformation of the denoised pupil size recordings. The relationship between the pupil response and the probability of seeing a stimulus was additionally analyzed.

Original data and results
Within this pilot study we obtained pupillographic data with sufficient quality from seven out of eight subjects (4 male, 4 female; age range from 27 to 56 years). Two of the subjects showed characteristic pupillary constriction and periods of pupillary fatigue waves, related to reduced vigilance during the perimetric session. Pupillary fatigue waves became more evident with increasing test duration.

Conclusion
Pupillary constriction and occurrence of fatigue waves are related to vigilance. IR-pupillography can be used to analyze vigilance and its effects in a commercially available perimeter in a highly standardized environment even under photopic conditions. This may allow to enhance the quality of visual field testing by terminating the perimetric session as soon as IR-pupillographic indicators of fatigue occur.

Reducing variability in visual field assessment for glaucoma through filtering using censored data

Authors: Lisha Deng, Shaban Demirel, Stuart K Gardiner
Institutional affiliation: Devers Eye Institute, Legacy Health, 1225 NE 2nd Ave, Portland, USA

Design and methodology: We have previously shown that filtering combining functional and structural test data can reduce variability and improve the accuracy of predicting the next test result while assessing glaucomatous visual field progression (Deng et al, ARVO 2014). Gardiner et.al. (Ophthalmology, 2014) reported that sensitivities estimated to be between 0dB and approximately 15-19dB during SAP perimetry are unreliable, and are only weakly correlated with true functional status within that range. We therefore extended the previous analysis using censored data. For analysis, we used 19dB as the lower limit of the reliable stimulus range of standard perimetry to improve the reliability of sensitivities, s.t. values <19dB were assigned 19dB. A 'cross-sectional' dataset consists of Humphrey visual field (VF) data (SITA Std, 24-2) and confocal scanning laser ophthalmoscopy (HRT) data (rim area in twelve 30º sectors) were used to derive a filter, containing eight predictors per location. A separate 'longitudinal' dataset which collected VF and HRT data from distinct participants as those in the cross-sectional data was used to test the filter. At each VF location per eye, the trend over time was modeled by a linear model (LM), and a non-linear model (NLM; rate of change worsening over time), using filtered or unfiltered data but with the last visit excluded. The standard deviations (SD) of residuals from the trends, and prediction errors (PE) for the last visit were compared between filtered and unfiltered data.

Original data and results: The cross-sectional dataset consisted of 1057 eyes of 637 participants, with 87.5% of eyes having contributed data from two or fewer visits. The longitudinal dataset consisted of 112 eyes of 62 participants with a minimum of 5 visits per eye. The longitudinal sequences had a mean follow-up time of 5.3 years, ranging from 1.9-11.5 years. Among all longitudinal sequences at the 52 VF locations, 2.6% had a second to last VF sensitivity below 19dB, and 2.5% had a last VF sensitivity below 19dB. The SD of the residuals using censored data at all 52 VF locations for both LM and NLM analyses were reduced by filtering ($p<0.001$). The PE were reduced by filtering at 47 and 52 VF locations ($p<0.05$) for LM and NLM analyses on censored data. Censoring data before filtering reduced the variability ($p<0.01$) at 41 and 40 VF locations for LM and NLM analyses.

Conclusion: Previously, we have concluded that our filter which incorporated data from both functional and structural tests provides better prediction of change in series of pointwise VF sensitivities when compared to using unfiltered data. Filtering is likely to yield clinical benefits by reducing the likelihood that a glaucomatous visual field will falsely be deemed progressing. Censoring data at 19dB provides an approach to reduce noise for the raw data, and filtering using censored data reduced the noise further. There are other ways to censor data to reduce noise. For example, instead of censoring data <=19dB to 19dB which will consistently cause an over-estimate of the true level of function, we could set those locations to be e.g. 10dB. However, setting them equal to 19dB makes the direction of the errors more predictable.

Poster Session II (3rd Floor)

Comparison of Kinetic Programs in Various Automated Perimetry

Authors: S Hashimoto 1, C Matsumoto 1, S Okuyama 1, E Arimura-Koike 2, H Nomoto 1, F Tanabe 1, T Kayazawa 1, M Eura 1, T Numata 1, S Shimada 1, Y Shimomura 1
Institutional affiliation:1Department of Ophthalmology, Kinki University Faculty of Medicine, Osaka-Sayama, Osaka, Japan
2 Department of Ophthalmology, Kinki University Faculty of Medicine, Sakai Hospital, Sakai, Osaka, Japan

Design and methodology: While static perimetry has currently become more popular in automated perimetry, kinetic perimetry remains important in evaluating visual fields (VF) affected by advanced glaucoma and retinal diseases. Manual Goldmann kinetic perimeter has been widely used in kinetic perimetry. On the other hand, various semi-automated and fully automated kinetic programs have been developed for kinetic perimeters. In this study, we evaluated the clinical usefulness of the kinetic programs in five available automated perimeters. Five kinetic programs were tested in this study including four semi-automated programs (HUMPHREY, the Humphrey Kinetic Test; OCULUS, Twinfield Kinetic Perimetry; GKP, OCTOPUS Goldmann Kinetic Perimetry; and KOWA, Kowa AP-7000 Isopter) and one fully automated program developed by us (Program K, OCTOPUS900). To test the programs, we used the results of Goldmann Kinetic Perimetry to create virtual patients with various types of VF defects including concentric contraction, a small central island with a separated temporal island remaining, only a temporal residual island and ring scotoma. The five kinetic programs were performed on the virtual patients to assess the VF loss using target sizes of V/4e, I/4e, I/3e, I/2e, and I/1e at two speeds of 3 and 5 degrees/sec.

Original data and results: Of the four semi-automated programs, OCULUS, GKP and KOWA could detect all types of VF loss. However, their results were considerably influenced by the examiner's skill and some isopters obtained by OCULUS and KOWA were incomplete indicating the possible problems in the isopter-drawing algorithms. We also faced difficulties in presenting some of the test targets when testing HUMPHREY. Program K could detect all types of VF defects except those in a divided field. The testing ranges of the peripheral VF for HUMPHREY, OCULUS, OCTOPUS and KOWA were 75°, 70°, 90 ° and 80°, respectively.

Conclusion: Semi-automated GKP and fully automated Program K are the potential kinetic methods with clinical usefulness.

Accuracy and Detection Rate of Increment vs. Decrement Stimuli in Patients with Glaucoma

Authors: Zhao, L, Komban S, Alonso JM, Zaidi Q, Dul M
Institutional affiliation: State University of New York, State College of Optometry

Purpose: Previous studies have shown that decrement stimuli are detected faster and more accurately than increment stimuli, when presented in noisy backgrounds (Komban et al., 2011). We investigated how these differences in detection time and accuracy are affected by age and by moderate glaucoma.

Methods: One eye of 10 glaucoma patients, 11 age-similar controls (50-83 y/o) and 3 young control subjects (23-25 y/o) were tested. Subjects were asked to count the number of light or dark targets superimposed on a white noise background as fast as possible. Each presentation contained 1-3 squared targets of 1° / side, located at random positions within the central 30° of the visual field. A total of 600-800 measures were collected per subject.

Results: We replicate previous findings (Komban et al., 2011) that darks are detected more accurately and faster than lights. We extend these findings by demonstrating that in controls, detection times increase with age, both for lights ($r=0.83$, $p<0.0001$) and darks ($r=0.85$, $p<0.0001$) but detection accuracy remains unchanged (lights: $r=0.37$, $p=0.18$; darks: $r=0.12$, $p=0.68$). When compared with controls, glaucoma patients showed a significant reduction of 7-11% in detection accuracy (normal/glaucoma, lights: 88.47% / 77.56%, $p=0.0035$, darks: 94.81% / 88.53%, $p=0.003$, Wilcoxon tests) but not detection time (normal/glaucoma, lights: 2.35 sec / 2.65 sec, $p=0.306$, darks: 1.64 sec / 1.87 sec, $p=0.307$, Wilcoxon tests).

Conclusions: Differences in the detection of darks and light are robust, and can be demonstrated over a wide range of ages and in patients with moderate glaucoma. The finding that patients with glaucoma show a 15% reduction in detection accuracy raises the question of whether a simple detection test could be used to monitor disease progression.

Perimetry Paper Session

Effect of response saturation on the test-retest correlation in damaged visual fields

Authors: Stuart K Gardiner1, Shaban Demirel1, Deborah Goren1, William H Swanson2
Institutional affiliation: 1Devers Eye Institute, Portland, USA; 2Indiana University, Bloomington, USA

Design and methodology: We have recently reported (Gardiner et al, Ophthalmology 2014) that the response probability to perimetric stimuli does not substantially increase with stimulus contrast below around 15-19dB in glaucoma. This makes such perimetric sensitivities unreliable. We suggest that this is consistent with the responses of retinal ganglion cells becoming saturated. However, there remains a weak test-retest correlation at such damaged locations, albeit with large variability (see e.g. Heijl et al, AJO 1989; or Artes et al, IOVS 2002). We propose that this is caused by differences in the asymptotic maximum response probability, which does not rise to 100% at some damaged VF locations.

In this study, a 'conventional' dataset was simulated using a full threshold algorithm, psychometric functions defined by a cumulative Gaussian and variability from Henson et al (IOVS 2000) capped below 19dB. 5000 test-retest series were simulated for each 'true' sensitivity from 1-35dB. For each possible 'test' sensitivity, we found the median and interquartile range (IQR) of retest sensitivities. This was then repeated but with the response probability remaining constant below some floor, for different floors between 1-19dB. The results were compared against patient test-retest data from the literature.

Original data and results: In the 'conventional' simulated dataset, for test sensitivities 0-19dB the retest IQR averaged 5.2dB. As the floor increased, the mean IQR over this range widened, and resembled published data more closely. Below that floor, the response probability was constant, yet the median retest sensitivity was still weakly related to test sensitivity. This is likely because the testing algorithm will repeatedly report higher sensitivities when the asymptotic maximum response probability is e.g. 70% than when it is 20%.

Conclusion: We suggest that above ~19dB, perimetry is measuring contrast sensitivity, whereas at more damaged locations, 'sensitivities' may instead reflect the maximum response probability. This could explain the high variability and weak test-retest correlation below 19dB reported in the literature.
Our simulation results are affected by the distribution of 'true' sensitivities, as well as the choice to apply a fixed response probability below the floor rather than introducing a possibly more realistic asymptotic maximum. However, our results demonstrate that these results in the literature are consistent with the response probability reaching an asymptotic maximum before 0dB. Response saturation may explain experimental results better than a model that ignores RGC response saturation.

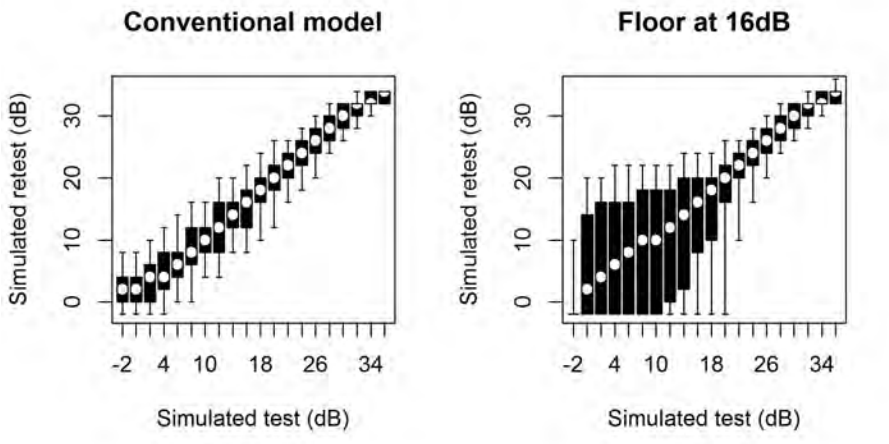

Visual field testing within complete spatial summation

Authors: Michael Kalloniatis and Sieu Khuu
Institutional affiliation: School of Optometry and Vision Science and Centre for Eye Health, University of New South Wales, NSW 2052, Australia

Design and methodology: Test size is a critical parameter for the early detection of eye disease. Dubois-Poulsen et al (Doc Ophthal 1959) first identified the importance of small test stimuli to enhance the detection of early visual field deficits in glaucoma patients. We wanted to design a visual field testing paradigm where test size was always within total spatial summation (Ricco's law) for all locations used in clinical perimetry. A number of parameters had to be empirically determined.

(A) Critical area (Ac): we determined this using the Humphrey Visual Field Analyser (HVFA) 30-2 paradigm for N=12 subjects. Also, we compared HVFA derived Ac results to those derived from a laboratory based testing protocol (N=28). We derived a testing template where test stimuli within the central 60-degree diameter (30-2 paradigm) would always be within total spatial summation.

(B) We had to develop a 'dB' value that would parsimoniously provide comparisons when testing with test sizes that are within total spatial summation. The new 'dB*' value equates spatial summation for test stimuli irrespective of size, normalizing them if test size is within Ricco's law.

(C) We used the normative data for 50 year-old from Heijl et al (Arch Ophthal 1987); compared it with our own data set (N=12). We showed that our data were not significantly different from Heijl's.

In order to apply the testing paradigm where test stimuli are within total spatial summation to disease populations, further empirical measures were required. First, we determined the effect on the Hill of Vision (HoV) using the new dB* data. Second, we determined the effect of optical blur (using +3.5DS blur) on the thresholds at different locations (both within and outside Ac). Finally, we empirically determined the mean deviation (MD) and pattern standard deviation (PSD) (from a large set of visual field results) to establish a correction factor to allow for comparison with the value provided by the HVFA. We used 12 normal subjects and 9 with optic nerve disease using the full threshold paradigm of the HVFA for test stimuli ranging from size I to V. Five of the 12 subjects undertook testing with optical blur. At least two threshold measurements were made for each condition. A total of 53 visual field results from a range of eye diseases were used to determine the correction factor for MD and PSD.

Original data and results: The HoV using the dB* measurement displays a similar shape but dramatic changes in overall location of each data set. Size I and II test stimuli largely overlap at all locations except in the fovea reflecting the fact that both are within the Ac at most locations within the 30-2 paradigm. Size III was only similar at peripheral locations when compared to sizes I and II; and size IV and V were always significantly below the dB* for sizes I and II. The effect of blur was similar in that when test stimuli are within total spatial summation, thresholds are affected, while outside (e.g., size IV/V), there was minimal impact. Finally, we established the correction factor for MD and PSD and used it to compare the results of the normal population and the two visual field paradigm (current vs test size within total spatial summation). When using the new paradigm, all 9 subjects with optic nerve disease provided worse results: MD change was -2.9→-4.7dB and the PSD change was 4.1→5.7.

Conclusion: We provide the theoretical and empirical evidence that the use of test stimuli that are within Ricco's spatial summation provide a mechanism to detect visual field loss at an earlier stage and provide a larger loss compared to current approaches.

Perimetry Paper Session

The gaze tracking and the test-retest reproducibility of visual field.

Authors: Yukako Ishiyama, Hiroshi Murata, Chihiro Mayama, Ryo Asaoka
Institutional affiliation Department of Ophthalmology, The University of Tokyo, Tokyo, Japan

Design and methodology: A novel method was developed to analyze the cumulative status of fixation during visual field (VF) measurement by integrating the gaze tracking record (IGT) on the Humphrey VF printout. IGT parameters were calculated as: average track failure time per stimulus (TFT), average movement between 1-2 degrees (move1-2), average movement between 3-5 degrees (move3-5) and average movement > 6 degrees (move>6). Humphrey VFs (24-2 and 10-2 SITA standard) were prospectively examined twice within the period of three months. The relationship of these parameters to VF reproducibility was investigated using second-order Akaike Information Criterion model selection, in which the mean absolute error of all 52 (in 24-2 VF) or 68 (in 10-2 VF) total deviation (TD) values of the two successive VFs was placed in one arm, and the average values of IGT parameters, Fixation loss (FL), False positive (FP), False negative (FN), mean deviation (MD) and pattern standard deviation (PSD) were placed in the other arm,.

Original data and results: 24-2 and 10-2 Humphrey VFs in 42 eyes of 42 glaucoma patients prospectively collected were analyzed. The MD values of the initial VFs were -10.8±7.5 (mean ± sd, [range: -28.2 to 2.1]) dB in 24-2 VF and -12.0±7.7 [27.2 to 1.4] dB in 10-2 VF. The selected models were: mean absolute error = 0.11*PSD + 3.6*TFT + 12.6*FN in 24-2 VF and mean absolute error = 0.087*PSD + 3.5*move3-5 in 10-2 VF ($p < 0.05$ for all of the coefficients).

Conclusion: Relationship was observed between IGT parameters and the reproducibility of VF results. Thus it is suggested that analyzing gaze tracking record quantitatively is useful for estimating the reliability of measured VF.

Visual Field Screening in Nepal Using an iPad to test Normal Controls, Persons with Glaucoma and Individuals with Diabetic Retinopathy

Authors: Chris A. Johnson, PhD, DSc1, Suman S. Thapa, MD, PhD2, Alan L. Robin, MD3
1 Department of Ophthalmology and Visual Sciences, University of Iowa Hospitals and Clinics
2 Nepal Glaucoma Eye Clinic, Tilganga Institute of Ophthalmology, Kathmandu, Nepal
3 Departments of Ophthalmology, University of Maryland and Johns Hopkins University

Purpose: To perform visual field screening in Nepal using a free program on the iPad, "Visual Fields Easy" to distinguish among visual field characteristics of healthy normal control eyes, glaucomatous eyes with visual field loss, and eyes with diabetic retinopathy that produce visual field loss.

Methods: The Visual Fields Easy program on the iPad was used to provide visual field screening to more than 450 eyes (about 200 healthy normal eyes, 200 glaucoma eyes, and 50 diabetic retinopathy eyes) in Nepal. The Visual Fields Easy program tests 96 visual field locations within the central 30 degrees, using a background luminance of 31.5 apostilbs (10 cd/m2), a size V target (when placed at 33 cm test distance) and a 16 dB suprathreshold static perimetry target for screening purposes. A red fixation point is presented to one corner of the display and one visual field quadrant is assessed, followed by movement of the fixation point to the other corners of the display to test the other three quadrants. Participants respond to detection of a stimulus by touching the display screen. False positive and false negative responses are also determined. Results of the Visual Fields Easy procedure were compared to the 24-2 SITA Standard findings on the Humphrey Field Analyzer for most of the participants. A comprehensive eye examination was used to establish the diagnosis.

Results: Correlations of missed targets on the iPad test with SITA Standard 24-2 MD and PSD results were better than 0.75 ($p<0.0001$) and 0.60 ($p<0.0001$), respectively. There were also strong correlations between the number of missed points on the iPad test and locations worse than the lower 5% probability level on the HFA Total Deviation (TD) plot ($r= 0.50$, $p< 0.0001$) and Pattern Deviation (PD) plot ($r = 0.675$, $p<0.0001$). Test time for the visual field screening was about 210 seconds (3 minutes, 30 seconds) per eye. Sensitivity and specificity for detecting early, moderate and advanced glaucomatous and diabetic retinopathy visual field loss will also be reported.

Conclusion: The "Visual Fields Easy" program on the iPad can quickly and easily identify moderate and advanced glaucoma, as well as diabetic retinopathy eyes that have visual field loss. This procedure appears to be a useful method of screening for common eye diseases for individuals with limited access to traditional health care. Refinements to the test strategy should reduce testing time and improve performance of this procedure (sensitivity, specificity and classification of visual field status). This procedure appears to be a good candidate for future approaches in telemedicine.

Perimetry Paper Session

A feasibility trial of the use of tablet devices for measuring central visual fields in age-related macular degeneration

Authors: Allison M McKendrick 1, Zhichao Wu 2, Robyn H Guymer2, Chang J Jung2, Jonathan K Goh 2, Lauren N Ayton 2, Chi D Luu 2, David J Lawson 3, Andrew Turpin 3
Institutional affiliation: 1. Optometry & Vision Sciences, The University of Melbourne, Australia
2. Centre for Eye Research Australia, The University of Melbourne, Royal Victorian Eye and Ear Hospital, Australia
3. Computing and Information Systems, The University of Melbourne, Australia

Design and methodology: We aimed to determine whether tablet computers are suitable for measuring visual field sensitivity in central vision. Adults with age--related macular degeneration (AMD) were studied to assess the utility in older adults with macular pathology. Our central visual field test was developed using PsyPad (Turpin et al, JoV, March 2014): an open--source platform for developing visual psychophysical tests on the iPad. An iPad3 was used (background set to 1.27 cd/m2). Test stimuli were Goldman Size III (scaled for a working distance of 50 cm) with a maximum and minimum luminance of317.50 cd/m2 and 1.52 cd/m2 respectively. Five visual field locations were tested: 0° (foveal), and four stimuli at 1° along the horizontal and vertical axis presented inside a red ring (radius of 3°) as a fixation target. A 4--2 staircase strategy was used to obtain the threshold measurements. Central retinal sensitivity was defined as the average measurements of these five points. Participants were trained on a practice test, then took 4 tests of one eye (in order to assess learning), followed by one test of their other eye. Participants also underwent central visual field assessment using the Macular Integrity Assessment (MAIA, CenterVue, Padova, Italy) microperimeter (37 point customised grid: central 5 points same as those on the iPad). The MAIA uses Goldmann size III stimuli (background of 1.27 cd/m2, maximum and minimum luminance of 318 cd/m2 and 1.37 cd/m2) and employs a 4--2 staircase strategy.

Original data and results: Thirty people with AMD participated (age range: 51--85 years, mean = 70.9). Twenty--five had intermediate AMD in both eyes and 5 had active CNV in one or both eyes. Each iPad test took on average 53.9 ± 7.5 seconds (range, 39 to 83 seconds). No significant learning effect was apparent across the 4 tests (P = 0.80). The coefficients of repeatability of central retinal sensitivity for each sequential examination pair of left eyes (test 1 vs test 2, test 2 vs test 3, and test 3 vs test 4) were 1.76, 2.20 and 3.02 dB respectively. The data of the first PsyPad examination of each eye was compared with microperimetry. Mean central retinal sensitivity did not differ using these methods (iPad: 25.7 ± 0.4 dB, microperimeter: 26.1 ± 0.4 dB, P = 0.09). Bland--Altman plots were used to examine the agreement between the methods, and showed no obvious relationship between the difference and magnitude. The 95% limits of agreement between the two methods were --4.12 to 4.92 dB (IQR: --0.8dB to 1.64dB).

Conclusion: In this pilot study, we only tested the very central visual field, however, testing a wider area of the visual field appears highly feasible. Participants anecdotally reported comfort and ease with the iPad testing platform. Tablet computers show promise as an inexpensive visual field screening device.

Reclaiming the Periphery – Kinetic automated perimetry (KAP) of the peripheral visual field compared to static automated perimetry (SAP) of the central visual field

Vera M Mönter,1 Paul H Artes,2 David P Crabb 1
1 Division of Optometry and Visual Science, City University London, London, UK
2 Ophthalmology and Visual Sciences, Dalhousie University, Halifax, Nova Scotia, Canada.

Design and methods: Peripheral vision is important for mobility, balance and guidance of attention, but standard perimetry of the central 30° examines less than 25% of the entire visual field. Here, we report on the relation between central and peripheral damage, and on test--retest variability of a fully automated kinetic test. In one eye of 24 patients with glaucoma (age median [range] 68 [59--83] y; MD
--8.0 [--16.3, +0.1] dB), a single isopter (III.1.e [15 dB] at 5°/s, 3 repetitions at each of 16 vectors, Fig 1b) was estimated (Octopus 900, Haag--Streit, Switzerland). Central fields were examined with the GATE strategy (24--2 test). Central and peripheral visual fields were measured twice on the same day.

Original data and results: MDs and mean isopter radii (MIR) were moderately related (Spearman's rho = 0.60, Fig 1a). The tests' retest variability appeared similar – 90% test--retest intervals ranged from --2.4 to 3.7° with the mean isopter radius (Fig 1c), and from --1.7 to a 3.1 dB with MD (Fig 1d).

Conclusion: Kinetic estimation of the peripheral visual field may add clinically relevant information to threshold perimetry of the central visual field. With an adaptive strategy, automated kinetic perimetry could be developed into a useful test of the peripheral visual field.

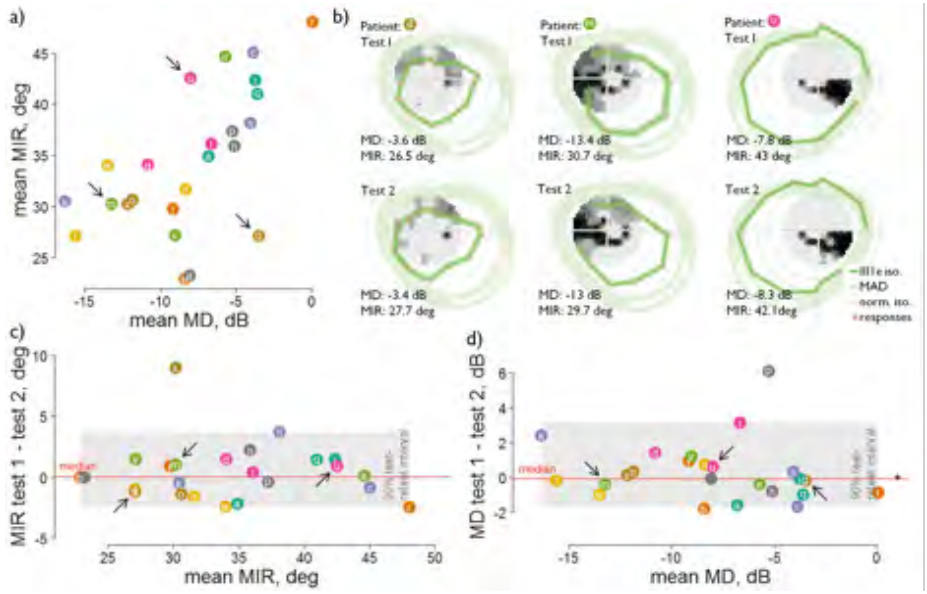

Fig 1: Patients are color--coded with small letter indices. a. Mean isopter radii (MIR) vs mean MDs b. Three examples of test--retest data. c, d. Bland--Altman plots of test--retest differences for mean isopter radii and MD.

Acknowledgements: This work was supported by an unrestricted research grant from MSD (DPC) and by a research grant from the Glaucoma Research Society of Canada (PHA). Haag--Streit International loaned an Octopus 900.

Structure - Function I Paper Session

Refining an Empirical Method for Estimating Ganglion Cell Axons from RNFL Thickness

Authors: William H. Swanson, PhD & Douglas G. Horner, OD PhD
Institutional affiliation: Indiana University School of Optometry, Bloomington, IN, USA

Design and methodology: Harwerth and colleagues developed an empirical model for estimating ganglion cell numbers from perimetric sensitivities based on data from non--human primates, and extended it to humans. They then developed a model for estimating axon numbers from retinal nerve fiber layer (RNFL) thicknesses. The current study refined their model for estimating axon numbers from RNFL thicknesses, by making mean number of neurons from RNFL more consistent with the mean number of ganglion cells from the perimetry model. Data analyzed were RNFL thicknesses (Stratus OCT 3.4), and visual field sensitivities (24--2 SITA Standard), for one eye each from 57 patients with glaucoma (mean ± SD = 65.4 ± 9.6 yrs) and 48 age--similar control subjects (61.9 ± 9.4 yrs) participating in a longitudinal study. Perimetric sensitivities were converted to estimates of ganglion cell numbers (RGCs) and RNFL thicknesses were converted to estimates of axon numbers (AXNs). These conversions were computed for the global RNFL versus the global visual field, and then separately for the inferior temporal (IT) and superior temporal (ST) sectors of the optic disc versus the corresponding visual field locations. The first refinement analyzed data from the control group, and reduced the assumed 0.9 μm axon diameter to make mean axon number from RNFL thickness equal to mean ganglion cell number from perimetry. The second refinement analyzed data from the patient group, and assessed potential effects of gliosis and axon shrinkage.

Original data and results: For pooled data from 105 patients and controls, all 105 participants had fewer AXNs than RGCs for ST, 100 had fewer AXNs than RGCs for IT, and 84 had fewer AXNs than RGCs for global measures (chi--squared > 35, $p < 0.0001$). For controls, on average RNFL yielded 11% more RGCs than AXNs for global measures, 56% more RGCs than AXNs for ST, and 86% more RGCs than AXNs for IT ($t > 2.8$, $p < 0.008$). Eliminating these differences required that axon diameter be reduced to 0.58 μm for ST and 0.48 μm for IT. When only the 13 symmetric locations for the IT and ST sectors were used (to reduce the contribution of macular ganglion cell axons for IT by excluding the location for IT that was closest to the fovea), diameters were 0.60 μm for ST and 0.72 μm for IT. With these new axon diameters, RGCs for patients were still greater on average than AXNs, by 23% for ST and 42% for IT. This difference could be reduced, but could not be eliminated, by reducing effects of gliosis when computing AXNs from RNFL. Axonal shrinkage was required to eliminate the difference in mean AXNs and RGCs for the patients.

Conclusion: The model for axon numbers from RNFL thicknesses systematically yielded lower numbers than did the model for ganglion cell numbers from perimetric sensitivities. This difference could be eliminated for controls by reducing assumed axon diameters. The axon diameters derived in this way were consistent with histological findings that human retinal ganglion cell axons have mean diameters from 0.46 μm to 0.73 μm depending on the retinal location of the cell body, with cell bodies near the fovea having the smallest axon diameters, and cell bodies in inferior retina having larger axons than cell bodies in superior retina. This finding is important because studies that have relied on the Harwerth model for estimating axon numbers from RNFL thickness may have systematically overestimated the amount of neural loss compared to perimetry, and the extent of this bias may vary with disc sector.

Correspondence Between Visual Field Test Results and GCL+IPL Thickness in the Maculae of Glaucomatous Eyes

Authors: Mariko Eura1, Chota Matsumoto1, Shigeki Hashimoto1, Sachiko Okuyama1, Sonoko Takada1, Eiko Arimura-Koike2, Hiroki Nomoto1, Fumi Tanabe1, Tomoyasu Kayazawa1, Takuya Numata1, Yoshikazu Shimomura1
Institutional affiliation: 1Department of Ophthalmology, Kinki University Faculty of Medicine, Osaka, Japan
2Department of Ophthalmology, Kinki University Faculty of Medicine, Sakai Hospital, Osaka, Japan

Design and methodology: In this study, we evaluated the correspondence between visual field (VF) test results and GCL thickness in the macula. Subjects were 32 normal eyes (52.5 ± 8.6 years) and 30 glaucomatous eyes (61.2 ± 9.5 years; 6 with preperimetric, 15 with early-stage, and 9 with moderate-stage glaucoma). Standard Automated Perimetry (SAP) using the 10-2 Humphrey Field Analyzer (HFA) SITA (size III) and full threshold (sizes III and I), and function-specific perimetry including 10-2 SWAP full threshold, 10-2 flicker perimetry on the Octopus 311 and 10-2 Humphrey Matrix ZEST using a temporal flickering frequency of 12 Hz were performed. Structurally, the GCL and inner plexiform layer (IPL) (GCL+IPL) thickness was measured by 3DOCT-2000 (Topcon). Evaluation was performed in the superior VF where more abnormalities were found this time. Corrections were made for any ganglion cell displacement from the photoreceptors in the fovea. The coefficient of determination (R2) for the correspondence between the VF results and the GCL+IPL thickness was separately calculated for each VF test at eccentricity 0°- 5°, 5°- 7°, and 7°-10°.

Original data and results: All the VF tests showed the closest correlation with the GCL+IPL thickness at eccentricity 5°-7°. The respective R2 values of linear and quadratic regressions at eccentricity 5°-7° were: 0.44 and 0.50 for HFA SITA (III), 0.46 and 0.52 for HFA FULL (III), 0.44 and 0.44 for HFA FULL (I), 0.47 and 0.47 for SWAP, 0.42 and 0.42 for Flicker, and 0.64 and 0.64 for Matrix. HFA SITA (III) and HFA FULL (III) had a higher R2 of quadratic regression than that of linear regression at all the eccentricities.

Conclusion: In the macula, SAP with size I and visual function-specific perimetry (especially Matrix) had more linear relationships with the GCL+IPL thickness than the often used SAP with size III.

Structure - Function I Paper Session

Temporal Retinal Nerve Fiber Trajectory Described by OCT and the Influence on the Humphrey 10-2 Test Points

Authors: F. Tanabe1), C. Matsumoto1), S. Okuyama1), S. Takada1), T. Numata1), T. Kayazawa1), M. Eura1), S. Hashimoto1), E. Arimura-Koike2), Y. Shimomura1)
Institutional affiliation: 1) Department of Ophthalmology, Kinki University Faculty of Medicine, 2) Department of Ophthalmology, Kinki University Faculty of Medicine, Sakai Hospital

Design and methodology: Individual difference in the anatomical positions of the optic disc and macula can cause variability in the retinal nerve fiber (RNF) trajectory. Using Spectral Domain OCT (SD-OCT) and Swept Source OCT (SS-OCT), we obtained a detailed description of the temporal RNF trajectories and investigated if these anatomical positions affected the arrangement of the 10-2 program.

Original data and results: Subjects were 12 eyes of 12 normal volunteers (SD, -2.9±2.7D, average age, 40.1 ± 10.1 years). Three-dimensional images were taken using SPECTRALIS® (SD-OCT) and Atlantis (SS-OCT), and were analyzed by Transverse Section Analysis (TSA) and EnView. Using the 3D OCT images, an image of the cross plane that fitted the inner limiting membrane (ILM) was reconstructed, and the RNF trajectories lying immediately under the ILM were depicted. With the reconstructed image, the disc-macula angle (the angle between the line connecting the fovea/disc and the horizontal line passing through the fovea), the macula-raphe angle (the angle between the horizontal line and the line connecting the fovea/temporal raphe), and the disc-raphe angle (the angle between the lines connecting the disc/fovea and the fovea/temporal raphe) were measured. To evaluate if the positions of the disc, macula, and temporal raphe affected the superior/inferior clusters, we detected the detailed location of the blind spot with an Octopus 900 custom test and superimposed the inverted 10-2 arrangement on the OCT image by matching the fixation point to the fovea and the blind spot to the disc.

Results: In all the subjects, both OCT devices could describe clearer temporal RNF trajectories than SLO. The respective average disc-macula, macula-raphe, and disc-raphe angles by SD-OCT and SS-OCT were 9.7˚±3.0˚ and 10.2˚±3.4˚, 0.9˚±2.9˚ and 1.1˚±2.6˚, and 169.4˚±2.5˚ and 168.6˚±3.6˚. In 9 (75%) subjects, the position of the disc was influenced by the test points near the disc in the inferior field. In 3 (25%) subjects, the position of the temporal raphe was influenced by the test points in the nasal inferior field.

Conclusion: The retinal horizontal raphe has an anatomical structure closer to the horizontal line passing through the fovea regardless of the positions of the disc and fovea. The anatomical structure of the disc and temporal raphe influenced the superior and inferior clusters in 75% of the subjects.

Customizing Structure--Function Maps of the Macular Region to Individuals

Authors: Andrew Turpin1, Juan A. Sepulveda2 and Allison M. McKendrick2
Institutional affiliation 1. Department of Computing and Information Systems (AT)
2. Department of Optometry and Vision Sciences (JAS and AMM) University of Melbourne, Australia.

Design and methodology: Drasdo et al (Vision Res 47, 2007) proposed a model to estimate the displacement of Retinal Ganglion Cells (RGCs) from their receptive fields (RFs) in the central retina. This model has been used in several recent structure--function studies of the macula. The model is based on population averages, however, and does not take into account data that may be unique to an individual.

In this work we adapt the approach of Drasdo et al to produce a structure--function mapping in the macular region that takes into account the foveal shape of an individual. In particular, we scale the estimated number of RGCs at any particular eccentricity based on the ratio of an individual's Ganglion Cell Complex thickness to a population average, as measured with the Spectralis OCT. We also depart from Drasdo's original model by estimating the average RGC count using Natural Neighbor interpolation of Curcio et al's tessellated RGC counts (Vision Research 29, 1989) rather than a single polynomial for all meridians.

Data was gathered on 9 participants with normal vision (aged 28 to 44 years) using the Spectralis SD--OCT. Custom macular structure--function maps were produced for each participant, and the estimated location of RGCs responding to a stimulus on the 10--2 pattern was measured.

Original data and results: The estimated RGC locations varied between individuals by about 1 degree centrally and about 0.5 degrees at an eccentricity of about 6 degrees in the superior retina and an eccentricity of about 8 degrees in the inferior retina. Variation was larger in the temporal retina than in the nasal retina.

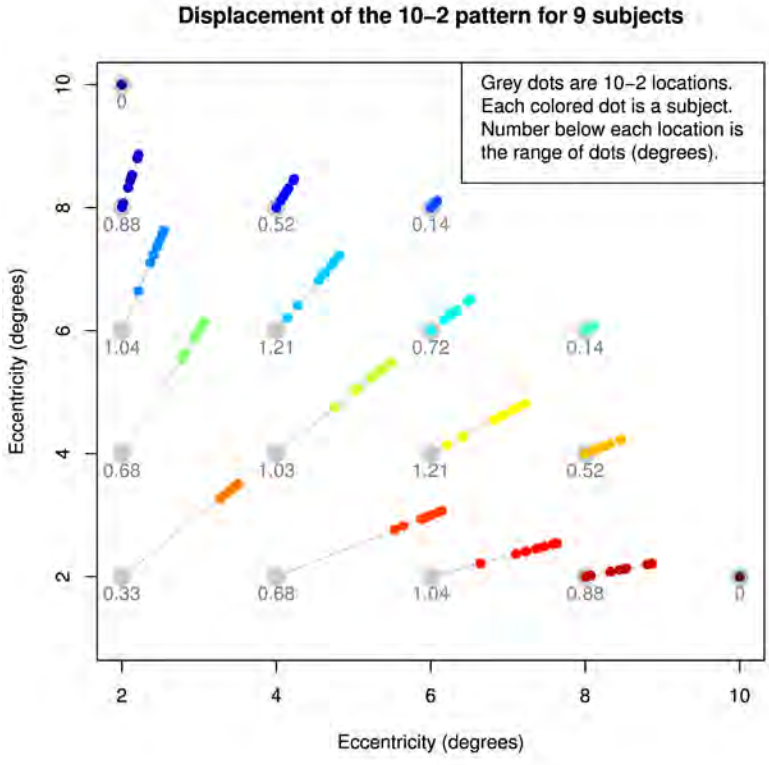

Estimated RGC displacement from 10–2 pattern locations in the temporal–superior retina

Conclusion: Using a structure--function mapping in the macula based on population averages could misestimate locations by over one degree. Customizing such a mapping to individual anatomy could lead to improved dia nostic power, customized visual field tests, and deeper understanding of glaucomatous progression.

Poster Session III (3rd Floor)

Moderator: Mitchell W Dul

Evaluation of two approaches for ocular magnification adjustment in circumpapillary retinal nerve fiber layer measurement

Authors: Kazunori Hirasawa1, Kazuhiro Matsumura2, Nobuyuki Shoji1,2
Institutional affiliation: 1. Orthoptics and Visual Science, Department of Rehabilitation, School of Allied Health Sciences, Kitasato University, Kanagawa, Japan and 2. Department of Ophthalmology, School of Medicine, Kitasato University, Kanagawa, Japan

Design and methodology: Traditionally, adjustment for ocular magnification was generally performed with Littman's methods by using individual corneal power, refraction, and axial length; not many devices were able to adjust for ocular magnification. However, it is now well established that optical coherence tomography (OCT) is used for the adjustment of ocular magnification to measure the circumpapillary retinal nerve fiber layer (cpRNFL) thickness. As an enhancement, in 2010, Kang et al. described new approach to adjust for ocular magnification using observed cpRNFL thickness. The aim of this study was to evaluate the cpRNFL thickness adjusted for ocular magnification by the existing Littman's method, which adjusts for the actual radius of scan circle on the disc, and by Kang's method, which adjusts for the observed cpRNFL thickness. One hundred and thirty-two eyes of 132 healthy participants were assessed with 3D-OCT 2000 (Topcon, Japan). First, baseline cpRNFL without adjustment for ocular magnification was imaged. Next, cpRNFL adjusted by Littman's method was imaged. Finally, cpRNFL thickness adjusted by Kang's method (Actual average cpRNFL thickness at 1.73 mm radius circle = 3.382*0.01306*[axial length - 1.82]*observed average cpRNFL) was calculated using baseline average cpRNFL thickness. The average cpRNFL thickness values adjusted by both methods were compared with absolute value of difference. To substantiate this study, randomly selected 45 eyes of 45 participants were imaged twice with baseline cpRNFL thickness, and the measurement error value was assessed for within subject standard deviation (2.77*Sw).

Original data and results: The limit of measurement error (2.77*Sw) was 5.2 μm. The average of absolute value of deference between the Littman and Kang method was 2.4 ± 2.4 μm. Of the total 132 eyes, 119 eyes (90.2%) were within the measurement error; however, 13 eyes (9.8%) exceeded this measurement error. The participants with refractive ametropia were mainly observed in these 13 eyes.

Conclusion: Using the Kang method, it was possible to adjust for ocular magnification in approximately 90% of our study participants. However, it is important to adjust this measurement for eyes with refractive ametropia, because the adjustment error was slightly larger than that obtained with the Littman method. This could possibly be attributed to the fact that Kang's method calculates only axial length and does not consider the calculated corneal refraction.

"Repeatability and agreement of peripapillary retinal nerve fiber layer and macular ganglion cell complex thickness using 2 different spectral domain optical coherence tomography devices."

Authors: 1, 2Juliane Matlach, 3, 4Martin Wagner, 3Uwe Malzahn, 1Winfried Göbel
Institutional affiliation: 1Department of Ophthalmology, University of Würzburg, Germany, 2NIHR Biomedical Research Centre for Ophthalmology, Moorfields Eye Hospital, London, UK, 3Institute of Clinical Epidemiology and Biometry, University of Würzburg, Germany, 4Comprehensive Heart Failure Center, University of Würzburg, Germany

Design and methodology: The purpose of this prospective cross-sectional study was to compare automated measurement of macular inner retina and peripapillary retinal nerve fiber layer (pRNFL) thickness using 2 different SD-OCT devices (Cirrus® HD-OCT and RTVue-100®), to assess repeatability of measurements and to evaluate agreement between both OCTs in preperimetric and perimetric glaucoma patients, patients with ocular hypertension, patients with idiopathic and atypical Parkinson´s disease and normal controls. One-hundred seventy-one eyes of 146 participants underwent successful pRNFL and macular scanning and automated measurement of ganglion cell layer + inner plexiform layer (GCL-IPL) using Cirrus or retinal nerve fiber layer + ganglion cell layer + inner plexiform layer (RNFL-GCL-IPL) using RTVue. Macular RNFL was added to the GCL-IPL thickness measured by Cirrus and was compared to the RNFL-GCL-IPL thickness of the RTVue in the corresponding Cirrus sectors. Intraclass correlation coefficient (ICC) was calculated to determine repeatability of 3 consecutive measurements, ICC and Bland-Altman analysis to assess agreement between OCTs, Pearson´s correlation coefficient to assess strength of linear correlation.

Original data and results: Intra-observer repeatability was excellent for average pRNFL thickness measurements with an ICC of 0.992 (95% CI 0.989-0.994) for Cirrus and 0.986 (95% CI 0.982-0.989) for RTVue (ICC > 0, P< 0.0001). Repeatability of macular RNFL-GCL-IPL complex was also excellent for average thickness for both OCT devices. ICC was 0.998 (95% CI 0.997-0.998) and 0.995 (95% CI 0.994-0.997) for Cirrus and RTVue, respectively (ICC > 0, P< 0.0001). Average macular RNFL-GCL-IPL and pRNFL thickness measured by the RTVue was generally thicker compared Cirrus. ICC values for agreement between both OCTs were generally good and ranged from 0.844 in the superior segment to 0.862 for the average macular RNFL-GCL-IPL thickness. For the pRNFL thickness, ICC ranged from 0.718 in the temporal quadrant to 0.958 in the inferior quadrant. The measurements from both devices correlated well with a Pearson´s correlation coefficient of 0.956 (P <0.0001) and 0.922 (P< 0.0001) for average pRNFL and macular RNFL-GCL-IPL thickness, respectively.

Conclusion: Measurement of pRNFL and macular RNFL-GCL-IPL thickness has a high degree of repeatability for both OCTs. Despite a high correlation between measurements and fair to excellent ICC-values representing a high consistency in the measurements of the two devices, RTVue measured a thicker macular RNFL-GCL-IPL and pRNFL thickness. To our knowledge, this is the first study reporting on a head-to-head comparison of inner macular thickness measurement using Cirrus and RTVue using an adjusted algorithm to have comparable measurements.

Poster Session III (3rd Floor)

Relationship between retinal nerve fiber layer thickness and peripapillary retinal tilt in healthy eyes

Authors: Yuya Kii, Takehiro Yamashita, Naoya Yoshihara, Minoru Tanaka, Kumiko Nakao, Taiji Sakamoto
Institutional affiliation Department of Ophthalmology, Kagoshima University Graduate School of Medical and Dental Sciences, Japan

Design and methodology: The purpose of this study was to investigate the relationship between the retinal nerve fiber layer (RNFL) thickness and the peripapillary retinal tilt (PRT) in young healthy eyes. Prospective observational cross-sectional study comprised 126 right eyes of 126 healthy young Japanese participants. RNFL thickness was assessed using the TOPCON 3D OCT-1000 MARK II RNFL 3.4 mm circle scan and divided into twelve clock hour sectors around the optic disc. The PRT was assessed using the RNFL circle scan B-scan images. The trajectory of the retinal pigment epithelium was fitted to sine curve using Image J and the amplitude of the sine curve was used for the degree of the PRT. The relationship between the sectoral RNFL thickness and the PRT or the axial length were investigated using the partial correlation analysis.

Original data and results: The mean axial length was 25.4 ± 1.5 mm and the mean PRT was 36.6 ± 17.5 pixels. The PRT was not significantly associated with the axial length ($R=0.11$, $p=0.21$). After excluding the effect of the axial length, the PRT was significantly and positively associated with the sectorial RNFL thicknesses of sectors 3, 7, 8, 9, 10 and 11 ($r=0.31\sim0.60$, $p<0.001$). After excluding the effect of the PRT, the axial length was significantly and negatively associated with the sectorial RNFL thicknesses of sectors 1, 2, 3, 4, 5 and 6 ($r=-0.33\sim-0.55$, $p<0.001$).

Conclusion: The temporal RNFL thickness increased as the peripapillary retinal tilt increased. The nasal RNFL thickness decreased as the axial length increased. The PRT and the axial length should be taken into account when determining the RNFL thickness.

Investigation of the retinal nerve structure in living human eyes

Authors: Muhammed S. Alluwimi, MS, William H. Swanson, PhD, Brett J. King, OD
Institutional affiliation Indiana University School of Optometry

Design and methodology: The organization of the retinal nerve fiber bundles in primates has been a controversial topic in the literature. Some studies reported that peripheral ganglion cells send their axons to bundles in deeper levels of the retinal nerve fiber layer (RNFL) than those closer to the optic disc. The second view was that peripheral ganglion cells send their axons to bundles at more superficial levels (vitro-retinal interface) of the RNFL. The third view suggested that there is no obvious organization for these bundles, and they take different paths based on embryological and chemical factors. To investigate the normal organization of the RNFL structure in living human eyes, 10 young volunteers free of eye disease, aged from 24 to 30 years, were imaged using dense vertical volume scans (with 30 microns spacing) with Spectralis OCT. Transverse analysis was used to evaluate RNFL structure at different depths from the vitreo-retinal interface to the scleral border of the RNFL. Montages of transverse images at specific distances from the vitreo-retinal interface were made from OCT dense
scans from several retinal regions corresponding to much of the central visual field tested with the 24-2. For explanatory analysis to evaluate the effect of aging versus glaucomatous damage on RNFL structure, the same dense scans were performed on five subjects selected from an ongoing glaucoma study: three patients with glaucoma (ages 68 to 73 years) with different patterns of glaucomatous visual field defect (paracentral, arcuate or nasal step), and two age-similar subjects free of eye disease on a recent exam (ages 60 to 65 years). To compare the patterns of damage to visual fields and RNFL, the patients were tested with Conventional Automated perimeter (CAP) using 24-2 SITA-Standard (size III stimulus) and Contrast Sensitivity Perimetry 2 (CSP-2, Horner et al., 2013 Optom Vis Sci. 90:466-74). Total Deviation values for visual field locations tested with CAP and CSP-2 were superimposed on the RNFL montages, with locations of stimulus presentations adjusted to account for displacement of Henle fibers.

Original data and results: Transverse analysis for all 12 people free of eye disease showed similar structure to the RNFL: as depth from vitreo-retinal interface increased, the orientations of bundles in the macula changed in a manner consistent with the second view in the literature. In the three patients with glaucoma, RNFL damage corresponded to visual field locations with abnormal total deviation for both CSP-2 and CAP. Narrow wedge defects in RNFL were seemed to be limited to certain depths of the RNFL, whereas wider wedges were seen at almost all depths. Moreover, there were asymmetries of RNFL patterns (superior versus inferior) in patients with glaucoma not seen in subjects free of eye disease.

Conclusion: Retinal nerve fiber bundles from ganglion cells farther from the disc were seen in depths closer to the vitreo-retinal interface of RNFL, while fibers 1-3 mm from the disc appeared to run to deeper levels. These findings may provide valuable information about the organization of retinal nerve fiber bundles in subjects free of eye disease. Different patterns of glaucomatous damage to the RNFL structure were seen with great detail, which may lead to a better understanding of the structurefunction relationship.

Poster Session III (3rd Floor)

Agreement of two methods of macula measurements by spectral-domain optical coherence tomography in glaucoma

Authors: Kimikazu Sakaguchi, Shinji Ohkubo, Sachiko Udagawa, Tomomi Higashide, and Kazuhisa Sugiyama
Institutional affiliation: Department of Ophthalmology and Visual Science, Kanazawa University Graduate School of Medical Science, Kanazawa, Japan

Design and methodology: To evaluate the agreement and correlation between the two methods of macula thickness measurements in the retinal ganglion cell layer plus inner plexiform layer (GCL+IPL) with spectral domain optical coherence tomography. A total of 118 open-angle glaucoma eyes (mean age: 55.9 ± 13.0 years old) were examined with a 3D OCT 2000 (Topcon Inc., Tokyo, Japan). Three-dimensional imaging data of the macula were obtained using a raster protocol of 512 ×128 (vertical × horizontal) within a cube of 7 × 7 mm (S-scan) and 12 × 9 mm (W-scan), from which a 6 × 6 mm area centered on the fovea were divided into 10 × 10 grids. Right eyes were analyzed, and eyes with Image Quality (IQ) <60 were excluded from the analysis. The GCL+IPL thickness was evaluated. The correlation and agreement of two scan methods were evaluated using Spearman's rank correlation coefficients and Bland-Altman analysis.

Original data and results: Six (5.1%) and 24 eyes (20.3%) were excluded because of poor IQ in S- and W-scans, respectively. Then, 93 eyes were analyzed. The mean GCL+IPL thickness in S- and W-scans were 61.2 ± 16.8 and 61.1 ± 17.5 μm in all 100 grids, 61.5 ± 16.1 and 61.4 ± 16.4 μm in the temporal superior quadrant, 65.2 ± 17.8 and 65.5 ± 18.0 μm in the nasal superior quadrant, 57.8 ± 14.0 and 57.4 ± 14.4 μm in the temporal inferior quadrant, and 60.1 ± 18.0 and 60.1 ± 18.1 μm in the nasal inferior quadrant, respectively. The correlation coefficients of thickness comparison between S- and W-scans were 0.965 and 0.950 to 0.978 in all 100 grids and 4 quadrants, respectively ($p<0.001$). No significant proportional bias was found in the Bland-Altman analysis.

Conclusion: Although a good IQ is hard to obtain in W-scan compared with S-scan, the mean GCL+IPL thickness of W-scan is strongly correlated to S-scan. W-scan is useful for measuring the macular GCL+IPL thickness in the central 6 x 6 mm area.

Macular Ganglion Cell Complex (GCC) and peripapillary Retinal Nerve Fiber Layer (RNFL) analysis with Spectral Domain OCT in the early diagnosis of glaucoma.

Authors: Zeppieri Marco MD PhD, Gismondi Maurizio MD, Tosoni Claudia MD, Salvetat M. Letizia MD, and Brusini Paolo MD.
Institutional affiliation: Azienda Ospedaliero- Universitaria Santa Maria della Misericordia, Department of Ophthalmology, Udine Italy.

Design and methodology: To evaluate the clinical usefulness of the spectral-domain optical coherence tomography (SD OCT) macular ganglion cell complex (GCC) analysis in detecting early structural damage in patients with ocular hypertension or early glaucoma.

Materials and Methods: We considered a total of 101 eyes of 101 patients (mean age 57.4; range 34-72) ; 61 with ocular hypertension (OHT) and 40 with early primary open-angle glaucoma (POAG) (Glaucoma Staging System 2 stage border and stage 1). A control group of 50 eyes from 50 healthy subjects (mean age 59.5; range 33-77) was also taken into consideration. Visual field examination were performed with the HFA 30-2 SITA Standard test. The examination of the GCC was performed with Spectral Domain OCT Nidek RS 3000, using the "Macula map" program (6 mm area). The peripapillary retinal nerve fiber layer (RNFL) thickness was analyzed with the "Disc map" program. The built-in database, which compares patient's data with normative values, was used to classify the results as normal, borderline or abnormal. The diagnostic accuracy of the macular GCC thickness analysis and the peripapillary RNFL thickness analysis was compared using the chi-square test.

Original data and results: In the normal group, specificity for the GCC analysis and the peripapillary RNFL thickness analysis was 100% and 96%, respectively (differences not statistically significant; $p>0.05$). In the early glaucoma patients the sensitivity of the GCC analysis and the peripapillary RNFL thickness analysis was respectively 67.5% and 62.5% when the borderline were considered as normal ($p>0.05$); and 92.5% and 90% when the borderline were included in the abnormal group ($p>0.05$). With regards to the 61 OHT eyes, the GCC analysis was abnormal in 10 cases (16.4%), borderline in 9 (14.7%) and normal in the remaining 42 eyes (78.8 %), whereas the peripapillary RNFL analysis resulted abnormal in 14 eyes (22.9 %), borderline in 13 eyes (21.3%), and normal in 34 cases (55.7%).

Conclusions: Macular GCC thickness and peripapillary RNFL thickness analysis with Spectral Domain OCT seem to provide clinical useful information regarding early structural damage in the management of ocular hypertension and early glaucoma patients, showing similar diagnostic accuracy. OCT parameters should be always considered in association with visual field results.

Structure - Function II Paper Session

Glaucoma morphological damage estimated from functional tests.

Authors: Manuel Gonzalez de la Rosa1, Silvia Alayon2, Marta Gonzalez-Hernandez3
Institutional affiliation1.- Department of Ophthalmology. La Laguna University. 2.- Department of Systems Engineering. La Laguna University. 3.- Hospital Universitario de Canarias.

Design and methodology: Aims: To compare direct morphological measurements with those deduced from functional tests (PATH method) and their respective diagnostic capacities. Methods: 111 normal eyes (examined twice) and 112 consecutive eyes with suspected or confirmed glaucoma (one eye per subject) were analyzed using Spark strategy (Oculus Easyfield Perimeter) and Cirrus Optical Coherence Tomography (OCT). Perimetric threshold values were used to deduce the thickness of the retinal nerve fiber layer (RNFL) in 25 sectors using equations obtained by stepwise multiple correlations. They were also used to derive a normalized value of the neuroretinal Rim Area, correcting for the influence of Optic Disc size and expressing the result as a percentage of the normal average relation. Similarly, we also attempted to deduce visual field defects from RNFL thickness data.

Original data and results: The correlation between the deduced and the measured RNFL thicknesses was: r=0.77 ($p<0.0001$, standard error (SE)=15.4 microns in normal and 15.1 microns in glaucomatous eyes) in the sector-by-sector comparison, and r=0.80 ($p<0.0001$, SE=10.0 microns in normal and 10.4 microns in glaucomatous eyes) for average RNFL thickness.
In normal subjects, the SE between 2 consecutive measurements of RNFL thickness was 13.2 microns in the sector-by-sector analysis and 4.6 microns for average RNFL thickness.
The correlation between the deduced and measured Rim Area was r = 0.87 ($P<0.000001$, SE = 6.7% in normal and 15.9% in glaucomatous eyes).

Receiver operating characteristic (ROC) analysis yielded the following areas, sensitivities and specificities:

- Measured Thickness: 0.89, 75.5%, 91.5%.
- Deduced Thickness: 0.91, 86.5%, 93.4%.
- Measured Rim Area: 0.96, 89.2%, 95.3%.
- Deduced Rim Area: 0.94, 82.9%, 96.2%.

On deducing mean deviation (MD) of the visual field from RNFL thicknesses, we obtained: r=0.77 ($p<0.0001$, SE=5.1dB) and the following ROC results.

- Measured MD: 0.89, 75.5%, 94.3%.
- Deduced MD: 0.90, 71.8%, 99.0%.

The relationship lost linearity when MD<-10dB. On excluding normal cases and those with profound defects, the number of pathologic points (NPP) presented poor correlation with real values (r= 0.43, p=0.002, SE=16.3 points).

Conclusion: Spark perimetry allowed deducing glaucomatous morphological alterations with significant accuracy. From morphological measurements we can estimate whether visual fields are normal or pathological, but not the topography of the defects.

Structure and function in multifocal pupillographic objective perimetry (mfPOP)

Authors: T Maddess, Kolic M, AYH Chain, AC James, CF Carle
Institutional affiliation: John Curtin School of Medical Research, Australian National University, Canberra, Australia.

Design and methodology: We compared peripapillary retinal nerve fibre layer (pRNFL) thickness and visual field changes detected using SITA SAP and multifocal pupillographic objective perimetry (mfPOP) in glaucoma. Structure-function correlations were computed for data from 25 open angle glaucoma patients and 24 normal control subjects. All subjects were tested using SAP thresholds and fields derived from three mfPOP stimulus methods: 1) LumBal: luminance-balanced bright yellow stimuli on a 10 cd/m2 yellow background; 2) Lum+Col: 150 cd/m2 green stimuli on 10 cd/m2 red; and 3) Lum+ColBal, which was the same as Lum+Col but with luminance balancing. Field data were grouped in arcuate clusters according to Stratus OCT sectors. Pearson correlation coefficients (r) by test region and arcuate cluster were calculated between mfPOP or SAP deviations and RNFL deviations from normative data.

Original data and results: The strongest correlations were observed in the superior-superotemporal sector in patients with at least one eye having severe glaucoma, defined as SAP MD<-12dB, yielding r = 0.95 and r = 0.91 for the mfPOP LumBal and Lum+Col protocols respectively; SAP r = 0.80 (all $p<0.05$). In those patients mean correlations across all test-points for both SAP and mfPOP SAP r = 0.54, LumBal r = 0.56, Lum+Col r = 0.52, Lum+ColBal r=0.44 ($p<0.05$). No significant correlation was observed in normal subjects for mfPOP or SAP. For all patient eyes taken together mean correlations were higher for SAP than mfPOP, however scatterplots of mfPOP/RNFL deviations were quite linear (Fig. A) while SAP data saturated (Fig. B).

Conclusion: For both methods the largest correlations with RNFL thickness corresponded to the inferior nasal field of more severely damaged eyes. Head to head comparison of mfPOP and SAP showed similar structure/function relationships. The correlations for the 3 mfPOP methods were similar to each other. This is the first study of the structure function relationship for mfPOP. This study did not use the newer mfPOP clustered volley method, which increases signal to noise ratios by 40% (see abstract of CF Carle et al.)

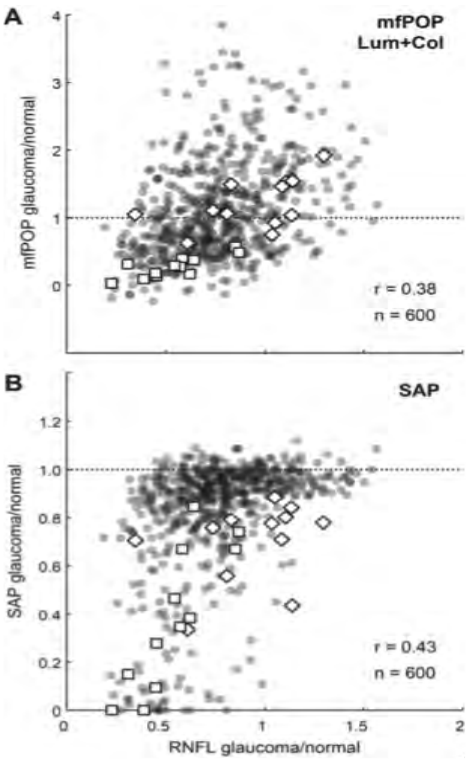

RNFL sector/Field test scatterplots for all glaucoma eyes (grey markers ●), and for a single glaucoma patient: left (◇) and right (□) eye. The other data points are semi-transparent grey, and therefore darker areas indicate higher concentrations of data.

Structure - Function II Paper Session

High resolution perimetry with 0.5 degree interval

Authors: T. Numata1, C. Matsumoto1, S. Okuyama1, S. Takada1, F. Tanabe1, S. Hashimoto1, M. Eura1, T. Kayazawa1, E. Arimura-Koike2, Y. Shimomura1
Institutional affiliation1Department of Ophthalmology, Kinki University Faculty of Medicine, Osaka-Sayama, Japan
2Department of Ophthalmology, Kinki University Faculty of Medicine, Sakai Hospital, Sakai, Japan

Design and methodology: We performed high resolution perimetry with 0.5 degree interval and investigated the detectability of glaucoma-related visual field defects in using various degree intervals. We also investigated correspondence between the function and the structure by comparing the high resolution visual field to the OCT image. Fifteen eyes of 15 patients with glaucoma (mean age: 63.3±6.0) and 11 eyes of 11 normal subjects (mean age: 63.5±2.7) were tested using the Octopus 900 custom test program three times. The test points were placed from the fixation point to the eccentricity of 30 degrees on the upper temporal meridian of 45 degrees with 0.5 degree interval. The blind spot was detected using another custom test with 1 degree interval grid. The corresponding retinal structure was examined using Cirrus HD-OCT with HD 5 Line Raster (1 line), 9 mm, High Definition Images. The visual field was superimposed on the OCT image by matching the blind spot to the optic disc and the fovea to the fixation point. The ganglion cell layer (GCL) + inner plexiform layer (IPL) thickness corresponding to each test point was measured manually. Within the eccentricity of 7 degrees, the location of the point was adjusted to correspond to the location of the retinal ganglion cell, taking into account its displacement near the fovea. In glaucoma cases, visual field profiles were plotted with various degree intervals, and then the mean defect (MD), the square root of loss variance (sLV) and the percentages of sensitivity loss were examined. And the correspondence of sensitivity to the GCL+IPL thickness was also investigated.

Original data and results: In our glaucoma cases, the detectability of visual field defects was decreased over 1.0 degree interval within the eccentricity of 10 degrees, 1.5 degree interval within 10.5-20 degrees. Within 20.5-30 degrees, the detectability of visual field defects wasn't decreased. In the eccentricity of more than 6.6 degrees, the dynamic range of GCL + IPL thickness was narrow. Therefore, the GCL + IPL thickness was not enough to reflect sensitivity differences. In the eccentricity of 6.6 degrees or less, the dynamic range of the GCL + IPL thickness was wide. In this area, functional changes were mostly corresponded with structural changes although we detected in some cases the functional changes preceded structural changes and in some others the structural changes preceded functional changes.

Conclusion: Detectability of visual field defects is greatly affected by the test resolution. The thickness of GCL + IPL can't reflect sensitivity loss in the eccentricity of more than 6.6 degrees.

Classifying normal and glaucomatous patients using machine learning methods

Authors: Hiroshi Murata1, Junkichi Yamagami2, Ryo Asaoka1
Institutional affiliation: 1Department of Ophthalmology, The University of Tokyo 2 JR Tokyo General Hospital

Design and methodology:
Various machine learning method, such as Random Forests, Supprot Vector Machine, Gradient Boosting methods, and logistic regression with automatic relevance determination were applied to discriminate between glaucoma and normal eyes using 151 OCT parameters including thickness measurements of circumpapillary retinal nerve fiber layer (cpRNFL) , the macular RNFL (mRNFL) and the ganglion cell layer-inner plexiform layer combined (GCIPL). The area under the receiver operating characteristic curve (AROC) was calculated adopting leave-one-out cross validation. For comparison, AROCs were calculated based on each one of the 151 OCT parameters.

Original data and results:
SD-OCT was conducted in 126 eyes of 126 open angle glaucoma (OAG) patients and 84 eyes of 84 normal subjects. Larger AROCs were obtained with machine learning classifiers, in particular with the Random Forests method. The AROC associated with the Random Forests method was 98.5 % [95% Confidence interval (CI): 97.1 - 99.9%]), which was significantly larger than the AROCs derived from any single OCT parameter (maxima were: 92.8 [CI: 89.4 - 96.2] %, 94.3 [CI: 91.1 – 97.6] % and 91.8 [CI: 88.2 – 95.4]% for cpRNFL-, mRNFL- and GCIPL-related parameters, respectively; $P < 0.05$, DeLong's method with Holm's correction for multiple comparisons). The partial AROC above specificity of 80%, for the Random Forests method was significantly larger than the AROCs of any single OCT parameter ($P < 0.05$, Bootstrap method with Holm's correction for multiple comparisons).

Conclusion:
It is useful to use machine learning classifiers, such as Random Forests method, in analyzing multiple SD-OCT parameters concurrently when diagnosing glaucoma.

Structure - Function II Paper Session

Fractal dimension analysis for circumpapillary retinal nerve fibre layer thickness profile in normal and glaucomatous eyes

Authors: Katsuyoshi Suzuki, Shinichiro Teranishi, Kayoko Tokuhisa, Rie Shiraishi, Chiemi Yamashiro, Takuya Mori, Koh-Hei Sonoda
Institutional affiliation: Department of Ophthalmology, Yamaguchi University Graduate School of Medicine

Design and methodology: Circumpapillary retinal nerve fibre layer (cpRNFL) thickness profile represent the unique distribution of retinal nerve fibre layer of each eye. Fractal dimension (FD) is one of the parameter of fractal characteristics of the data such as pattern or signal form images. The aim of this study was to investigate the complexity of cpRNFL thickness profile using fractal dimension analysis and to assess its relation with visual field (VF) parameter. cpRNFL thickness measured with spectral domain optical coherence tomography (SD-OCT: Cirrus OCT, Carl Zeiss Meditec) in ninety-seven eyes of normal subjects and glaucoma patients from Yamaguchi University Hospital dataset were reviewed retrospectively. VF mean deviation (MD) measured with standard automated perimeter (Humphrey Field Analyzer, Carl Zeiss Meditec) within six months at SD-OCT examination date were also reviewed. Glaucoma stages were classified with VF parameters such as normal (GHT: WNL; MD ≥ -6dB), glaucoma suspect (GHT: borderline; MD ≥ -6dB), early glaucoma (GHT: ONL; MD ≥ -6dB), middle glaucoma (GHT: ONL; -12dB ≤ MD < -6dB), or advanced glaucoma (GHT: ONL; MD < -12dB). FD of cpRNFL thickness profile was calculated using box-counting method in fractal analysis with ImajeJ software. Mean FD at each glaucoma stage was compared with each other. Correlations of FD or average cpRNFL thickness with MD were assessed using the Spearman rank correlation coefficient (r).

Original data and results: Mean FD (SD) of normal/glaucoma suspects (n = 52), early glaucoma (n = 17), or moderate/advanced glaucoma (n = 28) was 1.141(0.034), 1.104(0.030), 1.075(0.019) respectively, which was significantly different from each other (P<0.01). FD was correlated with MD (r = 0.73, P<0.001), and average cpRNFL thickness was correlated with MD (r = 0.66, P<0.001). In the data of early glaucoma and suspects (MD>-6 dB), both FD (r = 0.46 P<0.001) and average cpRNFL thickness (r = 0.33, P<0.001) were correlated with MD.
Conclusion (include a discussion about why this abstract is important): FD analysis was useful to evaluate the pattern change in cpRNFL thickness profile of glaucoma. FD is one of the characteristic parameters for assessing glaucoma severity.

The use of adaptive optics to improve the interpretation of OCT analysis of glaucomatous damage.

Authors: Hood, Donald C.1; Chen, Monica1; Chui, Toco Y.2; Alhadeff, Paula 2; Ritch, Robert2; Rosen, Richard B.2 ; Dubra, Alfredo3
Institutional affiliation: 1. Columbia University, New York, NY, United States. 2. New York Eye and Ear Infirmary, New York, NY, United States. 3. Ophthalmology, Medical College of Wisconsin, Milwaukee, WI, United States.

Design and methodology: To improve our understanding of glaucomatous damage as seen on OCT scans, 8 eyes of 8 glaucoma patients with clear arcuate defects within the macular region on 10-2 visual fields were tested using a prototype adaptive optics scanning light ophthalmoscope (AO SLO) system and optical coherence tomography system (OCT) (DRI OCT-1 and/or OCT-2000, Topcon, Inc). With the AO SLO system, images of the retinal nerve fiber (RNF) bundles were obtained in: 1. a 20° vertical by 1° horizontal region centered at the fovea and 2. a semicircular region about 1.5° wide near the edge of the optic disc. With OCT, 1. macular vertical line scans and 2. circular (1.7 mm radius) disc scans were obtained. AO SLO images were montaged, and then co-registered with a high quality fundus picture. The total deviation values of the 10-2 were superimposed after accounting for retinal ganglion cell displacement. The vertical line and circle OCT images were compared to the AO SLO images after aligning the images via corresponding blood vessels. Appropriate IRB approvals were obtained.

Original data and results: Vertical OCT and AO SLO images in regions of visual field defects: 1. All 8 vertical AO SLO images showed areas without any apparent RNF bundles within the region of the visual field defect. When the RNF bundles were absent, the OCT showed a thin (about 15 um) hypodense RNFL. This residual RNFL was typically not (7/8 eyes) included in the RNFL thickness by the OCT algorithm. 2. 7 of the eyes had AO SLO images with regions with RNF bundles of lower than normal contrast. In these cases, the OCT RNFL was thinner than normal and, in general (6/7 eyes), were included in the RNFL thickness by the OCT algorithm. 3. Reasonably normal RNF bundles also were seen within regions of missing or abnormal bundles in 2 eyes and these regions were difficult to discern on OCT images. Peripapillary OCT and AO SLO images in disc locations corresponding to visual field defects: 1. In all eyes, RNF bundles were present, but markedly reduced in contrast in the affected portion of the disc. A complete loss of RNF bundles, if present, was only seen in very small regions. The corresponding regions on the OCT images were hypodense, but, in general (7/8 eyes), were included within the RNFL thickness by the algorithm. 2. In 2 eyes, bundles with reasonably good contrast were seen within the abnormal region.

Conclusion: The findings have implications for detecting glaucomatous damage with OCT. First, if the OCT RNFL region is hypodense, then a normal OCT peripapillary RNFL thickness does not necessarily imply a normal RNFL. Second, residual RNFL thickness in regions of complete loss of RNF bundles may or may not be included by the OCT algorithm. Third, small local regions of relatively preserved RNFL can be missed on OCT scans. Finally, all three of these finding will contribute to the variability seen in attempts to correlate structure (OCT RNFL thickness) and function (visual field loss).

Imaging & Population Studies Paper Session

Retinal vessel density is strongly correlated with circumpapillary RNFL at a 3.4mm diameter circle

Authors: Clemens Vass 1, Ivania Pereira1,2, Stephanie Weber1, Stephan Holzer1, Hemma Resch1, Georg Fischer2
Institutional affiliation: 1. Department of Ophthalmology & Optometry, Medical University Vienna, Vienna, Austria
2. Center for Medical Statistics Informatics and Intelligent Systems, Section for Medical Information Management and Imaging, Medical University Vienna, Vienna, Austria

Design and methodology: Circumpapillary RNFL thickness of 106 healthy volunteers was measured using FD-OCT. We assessed the thickness and position of circumpapillary retinal vessels at a 3.4mm diameter circle using the SLO fundus image. The individual retinal vessel positions and thickness values were integrated in a 256-sector retinal vessel density profile (RVD profile) using a Gaussian-shaped function. We calculated the intrasubject and intersubject correlations of RVD with the 256 sector RNFL profile, as well as an intersubject regression analysis with the RVD as independent and the RNFL as the dependent variable. This regression was calculated separately for all 256 sectors.

Original data and results: All individual RVD profiles showed a strong positive correlation with the respective RNFL profile (mean 0.769 ±0.117). Intersubject linear regression analysis resulted in a significant Pearson correlation coefficient in 96% of the sectors (mean 0.423 ±0.121, maximum 0.652) and a positive slope of the regression formula for all significant sectors. Using the regression formula and the RVD data to normalize the RNFL for an average RVD profile, reduced the mean coefficient of variance from 18% to 16%, with a maximum reduction in the temporal superior area from 19% to 15%.

Conclusion: Retinal blood vessels may be used as biomarkers for the physiologic differences in RNFL distribution. In future normative data may take these biomarkers into account and we present a method how to do so. Theoretically this would improve sensitivity and specificity of RNFL measurement.

Relationship between position of retinal nerve fiber layer defect and retinal artery trajectory in normal tension glaucoma

Authors: Takehiro Yamashita1, Koji Nitta2,3, Kazuhisa Sugiyama3, Taiji Sakamoto1
Institutional affiliation 1. Kagoshima University Graduate School of Medical and Dental Sciences 2. Fukui-ken Saiseikai Hospital 3. Kanazawa University Graduate School of Medical Science

Design and methodology: The purpose of this study was to quantify the retinal artery trajectory (RAT) and to investigate the relationship between the RAT and the position of the retinal nerve fiber layer defect (NFLD) in normal tension glaucoma (NTG). Retrospective observational study comprised 88 eyes of 88 NTG patients who had wedge-shaped NFLDs. The RAT and the position of NFLD were assessed using the fundus photographs. The supra and infra temporal retinal artery was plotted on a color fundus photograph and fitted to second degree polynomial (ax*x/100+bx+c) using Image J. The coefficient 'a' was used for the degree of the RAT. On the red free fundus photographs, the proximity of the NFLD to the fovea (supra-NFLD-angle, infra-NFLD-angle) were determined. The relationship between the RAT and the supra-NFLD-angle or the infra-NFLD-angle was investigated using the linear regression analysis.

Original data and results: Fifty six eyes had supra temporal NFLD and 69 eyes had infra temporal NFLD. The mean RAT was 0.232 ± 0.073, the mean supra-NFLD-angle was 50.3 ± 12.6 degrees and the infra-NFLD-angle was 34.6 ± 11.3 degrees. The RAT was significantly associated with the supra-NFLD-angle (R=-0.27, p=0.041), but not significantly associated with the infra-NFLD-angle (R=-0.06, p=0.61).

Conclusion: Localized supra temporal NFLDs were close to the fovea as the retinal artery shifted toward the fovea in NTG patients. The trajectory of the temporal retinal artery can be a good predictor of the proximity of the NFLD to the fovea.

Imaging & Population Studies Paper Session

Glaucomatous retinal nerve fiber layer patterns of loss identified by unsupervised Gaussian mixture model with expectation maximization (GEM) analysis

Authors: Siamak Yousefi1, Michael H. Goldbaum1, Linda M. Zangwill1, Felipe A. Medeiros1, Robert N. Weinreb1, Jeffrey M. Liebmann2, Christopher A. Girkin3, and Christopher Bowd1

Institutional affiliation 1Hamilton Glaucoma Center and the Department of Ophthalmology, University of California San Diego, CA, 2Department of Ophthalmology, New York University, NY, 3Department of Ophthalmology, University of Alabama, Birmingham, AL

Design and methodology: The purpose of this study was to automatically identify glaucomatous defect patterns from abnormal and normal retinal nerve fiber layer (RNFL) thickness measurements. An unsupervised Gaussian mixture model using the expectation maximization (GEM) method was employed to find the structure hidden in cross-sectional abnormal and normal RNFL thickness measurements. 500 models were trained and the model with the best average combination of sensitivity and specificity was chosen. The best model generated 3 clusters. RNFL thickness of the centroid of each cluster was examined to assign clusters as glaucomatous and normal. Principal component analysis was then used to decompose each cluster into several axes and display the glaucomatous pattern of RNFL thickness identified for each axis within the glaucomatous clusters, using simulated deviation plots. The simulated deviation plot is a 16-dimensional vector obtained by subtracting the RNFL thickness vector at the centroid of the normal cluster N from the absolute RNFL thickness vector at the centroid of the two glaucomatous clusters and then representing structural defects as plots at -2, 0 (cluster centroid) and +2 standard deviations (SD) along each of the axes. Resulting patterns were overlaid on en face images to allow visualization of the location of defect patterns.

Original Data and Results: RNFL thickness measurements were obtained using the Spectralis RNFL Circle Scan configuration from 2,326 eyes of 1,202 participants in the Diagnostic Innovations in Glaucoma Study (DIGS) and the African Descent and Glaucoma Evaluation Study (ADAGES). 709 eyes had at least one sector of six (ST, T, IT, IN, N, SN) with RNFL thickness outside of normal limits and 1,617 eyes had all sectors within normal limits. Sensitivity was 72% for placing abnormal RNFL thickness measurements in one of the two abnormal clusters and specificity was 84% for placing normal RNFL thickness measurements in the normal cluster.

Conclusion: GEM separated RNFL thickness measurements from abnormal and normal eyes with reasonable sensitivity and specificity. Distinctly different patterns of glaucomatous RNFL defects were identified. This method likely can provide a good environment of axes for detecting glaucomatous progression.

Measuring the amount of hemoglobin in the neuroretinal Rim using stereoscopic color fundus images.

Authors: Cristina Pena-Betancor1, Marta Gonzalez-Hernandez1, Jose Sigut2, Manuel Gonzalez de la Rosa3,
Institutional affiliation1.- Hospital Universitario de Canarias. 2.- Department of Systems Engineering. La Laguna University. 3.- Department of Ophthalmology. La Laguna University.

Design and method: The Laguna ONhE method1 was used to calculate the amounts of hemoglobin (Hb) in sectors of the optic disc from stereoscopic color fundus images. The images were obtained simultaneously using the non-midriatic Wx 3D camera (Kowa) with manual Cup and Rim delimitation. This method was compared with an automatic boundary delimitation method of Disc, Cup and Rim using image segmentation based on color patterns. We analyzed 91 normal eyes, 34 consecutive eyes with ocular hypertension, suspected or early glaucoma and perimetric mean deviation (MD) >-3dB (HSE group), and 39 eyes with moderate or confirmed glaucoma. In addition, the eyes were studied using Cirrus OCT (Zeiss) and Spark strategy (Oculus Easyfield Perimeter).

Original data and results: Glaucomatous eyes presented significantly less Hb than normal eyes for all sectors of the Rim ($p<0.001$) except the temporal sector ($p>0.22$), especially the inferior and superonasal sectors ($p<0.0001$). In the HSE group, we detected significant anomalies in topographic Hb distribution, manifesting in abnormal Glaucoma Discriminant Function (GDF). This index proved more sensitive on combining it with morphological data (GDFc). Visual field defects correlated better with Hb amounts than with the area of diverse sectors of the Rim ($p<0.01$) except in the central visual field ($p=0.43$). Vertical Cup/Disc (C/D) ratios obtained with OCT and Kowa showed a correlation of $r=0.75$. C/D estimated from Hb correlated with those of OCT ($r=0.68$) with Kowa ($r=0.82$) and with the average OCT&Kowa ($r=0.80$). Rim Areas (RA) obtained with OCT and Kowa presented a correlation of $r=0.56$. RA estimated from Hb correlated with those of OCT ($r=0.67$) and Kowa ($r=0.74$) and with the average OCT&Kowa ($r=0.80$).

For specificity near 95%, receiver operating characteristic (ROC) areas and sensitivities were as follows:
Manual boundary (all cases): C/D (0.80, 56.2), RA (0.65, 26.0), GDF (0.87, 53.4), GDFc (0.86, 63.0).
Manual boundary (HSE): C/D (0.72, 41.2), RA (0.57, 8.8), GDF (0.81, 41.2), GDFc (0.79, 48.5).
Automatic boundary (all cases): C/D (0.80, 54.2), RA (0.66, 23.6), GDF (0.88, 61.1), GDFc (0.92, 68.1).
Automatic boundary (HSE): C/D (0.72, 41.2), RA (0.57, 8.8), GDF (0.86, 52.9), GDFc (0.90, 57.2).

Conclusion: Simultaneous stereoscopic images obtained with the Kowa camera allow Cup and Rim segmentation applicable to the topographic measurement of Hb without recourse to any other instrument. Automatic segmentation also yielded useful results. In many glaucoma cases the remaining Rim has insufficient perfusion. C/D ratio seems to have greater diagnostic capacity than RA using stereoscopic images. The diagnostic capacity of Laguna ONhE GDF index and of C/D ratio showed no significant differences, but the combination of GDF with morphological indices may be advantageous.

1.- Gonzalez de la Rosa M et al. Invest Ophthalmol Vis Sci. 2013;54: 482-9.

Imaging & Population Studies Paper Session

Measuring the amount of hemoglobin in the neuroretinal Rim using color images and OCT.

Authors: Marta Gonzalez-Hernandez, Erica Medina-Mesa, Francisco Fumero-Batista, Manuel Gonzalez de la Rosa
Institutional affiliation1.- Hospital Universitario de Canarias. 2.- Department of Systems Engineering. La Laguna University. 3.- Department of Ophthalmology. La Laguna University.

Design and methodology: The Laguna ONhE1 method was used to calculate the amount of hemoglobin (Hb) in the optic nerve using color images obtained with a Visucam fundus camera (Zeiss). The images were made to coincide with boundary Cup and Disc images obtained by OCT Cirrus (Zeiss), which allowed us to calculate the amount of hemoglobin in the Cup and in the sectors of the Rim. We analyzed 100 normal eyes and 121 consecutive eyes with suspected or confirmed glaucoma (one eye per subject, average mean deviation MD=-7.7dB). Subjects were also studied using Spark strategy (Oculus Easyfield Perimeter).

Original data and results: In patients with suspected and confirmed glaucoma, the amount of hemoglobin was significantly lower than controls in all Rim sectors ($p<0.001$), especially the inferior and superonasal sectors ($p<0.0001$). The difference was less pronounced in the temporal sector ($p=0.049$).
On the receiver operating characteristic (ROC) analysis, the best diagnostic indicators were vertical cup/disc ratio (C/D), OCT Rim Area, Glaucoma Discriminant Function (GDF) of the Laguna ONhE program and Spark pattern standard deviation (PSD), without significant differences. Combining Laguna ONhE-GDF with Spark-PSD showed the highest sensitivity and ROC area.

	C/D Ratio	Rim Area	GDF	PSD	PSD&GDF
ROC AREA	0.89	0.90	0.87	0.93	0.96
SPECIFICITY	96.0	95.0	95.0	95.0	95.0
SENSITIVITY	70.2	71.9	62.8	60.3	83.5

Visual field defects showed better correlation with the amount of hemoglobin than with the area of the respective Rim sectors, with significant differences in various sectors.

Conclusion: Dr. Denniss' suggestion2,3 that the Laguna ONhE method should be associated with Cup and Rim measurements has been achieved. The results indicate that the remaining Rim has insufficient perfusion in many cases of glaucoma. The combination of Laguna ONhE GFF with Spark PSD showed high diagnostic capacity.

1.- Gonzalez de la Rosa M et al. Invest Ophthalmol Vis Sci. 2013;54: 482-9.
2.- Denniss J. Invest Ophthalmol Vis Sci. 2013;54:1515
3.- Gonzalez de la Rosa M et al. Invest Ophthalmol Vis Sci. 2013;54:2011-2

Trends in visual field defect severity at the point of diagnosis in large scale data from clinics in England

Authors: Trishal Boodhna; Richard A. Russell, David P. Crabb.
Institutional affiliation: Division of Optometry and Visual Science, City University London.

Design and methodology: It is possible to audit the performance of glaucoma related health care delivery by collecting large scale visual field data from the clinics that provide these services. Given the size of the data available, it is possible to examine for trends that exist in terms of glaucoma diagnosis and management within the service. We examine the hypothesis that glaucoma patients are more likely to be diagnosed with less severe VF damage in recent years when compared to the past. We retrospectively interrogated approximately 500,000 Humphrey SITA VFs that were undertaken at four regionally different glaucoma clinics in England between 1998 and the end of 2012. As a surrogate for a diagnosis of glaucoma with VF loss, patients were required to have a Humphrey mean deviation (MD) outside 95% normative limits in at least one eye and to have undertaken at least two VFs at their glaucoma clinic. The patients worst eye MD (WEMD) at their first visit to the clinic was used to represent the degree of VF loss at initial presentation; these were then simply stratified as 'early' glaucoma (better than -6dB), 'moderate' glaucoma (-6 to -12dB) and 'advanced' glaucoma (worse than -12dB). Three equal time periods (1998-2002, 2003-2007 and 2008-2012) were then specified and the proportion of patients defined with early, moderate and advanced glaucoma during these time periods were examined for significant change. In addition, trend analyses of WEMD against the date of initial presentation over the 15 year period were undertaken.

Original data and results: A total of 26,131 patients were examined as part of this study. Between 1998-2002, 43.0% were identified with early VF loss compared to 49.5% between 2008-2012 ($P<0.001$). Between 1998-2002, 28.9% were identified with severe VF loss compared to 22.2% in 2008-2012 ($P<0.001$). Trend analyses indicate that the level of VF loss at the point of diagnosis is improving by about 1dB every 10 years (0.11dB per year across the study period [95% confidence interval: 0.09-0.13 dB per year])

Conclusion: In the population of glaucomatous patients who present with VF loss at diagnosis there is a trend for less severe VF defects. Whether these statistically significant improvements are of a substantial magnitude to conclude that the health service delivery of this aspect of glaucoma is improving is a subject for debate and health economic analyses. Nevertheless, a significant proportion of patients are still presenting at glaucoma clinics with severe VF loss in at least one eye.

Imaging & Population Studies Paper Session

Tell us where you live and we will tell you something about your visual fields

Authors: David P. Crabb ; Richard A. Russell, Stefano Ceccon
Institutional affiliation: Division of Optometry and Visual Science, City University London.

Design and methodology: We use modern geodemographic tools to interrogate large volumes of patient data to examine factors that are associated with late presentation of visual field loss in glaucoma. Over 500,000 Humphrey visual fields (VFs) recorded in four regionally different glaucoma clinics/services in England (Cheltenham, Huddersfield, London and Portsmouth) in the last decade were retrospectively investigated. Measures for late presentation of glaucoma were estimated by a patient's VF damage (mean deviation [MD] at first visit). Socioeconomic status and consumer/community segmentation data was defined by patients' postcodes (ZIP codes) using the IMD (Index of Multiple Deprivation) and ACORN (A Classification Of Residential Neighbourhoods) geodemographic tools.

Original data and results: Data from 57090 patients were analysed. There were strong links between geodemographic measures of socioeconomic status and later presentation of VF loss. There was significant correlation between MD at presentation and IMD score (rho = -0.20; $p < 0.0001$; partial correlation corrected for age); geodemographic maps highlight this relationship. (Figure: Maps of central London showing severity of VF loss and IMD score. Darker areas correspond to areas where patients live that present with more severe disease and have worse socioeconomic status. Note the striking spatial concordance between the shading of these maps.) Patients from the least deprived areas, on average, are predicted to present with significantly less MD damage (MD = -5 dB; 95% confidence interval [CI] = -4 to -6 dB) than patients from the most deprived regions (MD = -9 dB; 95% CI = -8 to -10 dB). Other geodemographic maps reveal relationships between late detection of VF loss and proximity to primary health care providers (optometrists). ACORN Segmentation of communities, including knowledge of consumer/lifestyle behaviour, suggests methods by which vulnerable groups could be targeted for screening or enhanced public health campaigns.

Conclusion: Large scale visual field data from glaucoma clinics is a valuable resource that can be used to reveal associations between socioeconomic status and late presentation of glaucoma. Interactive geodemographic mapping tools can help illuminate public health and service delivery requirements for glaucoma.

MD at diagnosis

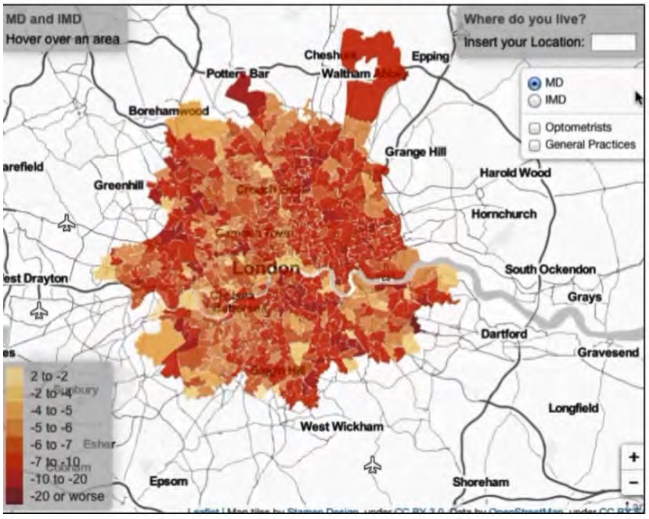

IMD Score